

Neurobiology:

Therapeutic molecules and endogenous ligands regulate the interaction between brain cellular prion protein (PrP^C) and metabotropic glutamate receptor 5 (mGluR5)

Laura T. Haas, Mikhail A. Kostylev and
Stephen M. Strittmatter
J. Biol. Chem. published online August 22, 2014



Access the most updated version of this article at doi: [10.1074/jbc.M114.584342](https://doi.org/10.1074/jbc.M114.584342)

Find articles, minireviews, Reflections and Classics on similar topics on the [JBC Affinity Sites](#).

Alerts:

- [When this article is cited](#)
- [When a correction for this article is posted](#)

[Click here](#) to choose from all of JBC's e-mail alerts

This article cites 0 references, 0 of which can be accessed free at
<http://www.jbc.org/content/early/2014/08/22/jbc.M114.584342.full.html#ref-list-1>

Therapeutic molecules and endogenous ligands regulate the interaction between brain cellular prion protein (PrP^C) and metabotropic glutamate receptor 5 (mGluR5)*

Laura T. Haas^{1,2,3}, Mikhail A. Kostylev^{1,3}, and Stephen M. Strittmatter¹

¹ Cellular Neuroscience, Neurodegeneration and Repair Program, Department of Neurology, Yale University School of Medicine, New Haven, Connecticut, USA.

² Graduate School of Cellular and Molecular Neuroscience, University of Tuebingen, Tuebingen, Germany.

³ L.T.H. and M.A.K. contributed equally to this work.

* Running title: *Therapeutic modulation of the PrP^C-mGluR5 interaction*

Correspondence should be addressed to Stephen M. Strittmatter, Cellular Neuroscience, Neurodegeneration and Repair Program, Yale University School of Medicine, 295 Congress Avenue, New Haven, CT 06536. E-mail: stephen.strittmatter@yale.edu.

Keywords: Alzheimer's disease, cellular prion protein, metabotropic glutamate receptor 5, therapeutic modulation, protein-protein interaction

Background: Amyloid- β oligomers trigger Alzheimer's disease pathophysiology via interaction of cellular prion protein (PrP^C) with metabotropic glutamate receptors 5 (mGluR5).

Results: PrP^C-region 91-153 interacts preferentially with the activated conformation of mGluR5.

Conclusion: Antibodies against PrP^C-region 91-153 and agonist/antagonist-driven mGluR5-conformations regulate the PrP^C-mGluR5 interaction.

Significance: These findings have therapeutic implications for Alzheimer's disease by identifying compounds that modulate the PrP^C-mGluR5 interaction.

ABSTRACT

Soluble Amyloid- β oligomers (A β) can trigger Alzheimer's disease (AD) pathophysiology by binding to cell surface Cellular Prion Protein (PrP^C). PrP^C interacts physically with metabotropic glutamate receptor 5 (mGluR5), and this interaction controls the transmission of neurotoxic signals to intracellular substrates. Since the interruption of the signal transduction from PrP^C to mGluR5 has therapeutic potential for AD, we developed assays to explore the effect of endogenous ligands, agonists/antagonists and antibodies on the interaction between PrP^C and mGluR5 in

cell lines and mouse brain. We show that the PrP^C segment of aa 91-153 mediates interaction with mGluR5. Agonists of mGluR5 increase the mGluR5/PrP^C interaction, while mGluR5 antagonists suppress protein association. Synthetic A β promotes the protein interaction in mouse brain and transfected human embryonic kidney-293 (HEK-293) cell membrane preparations. Critically, the interaction of PrP^C and mGluR5 is dramatically enhanced in the brains of familial AD transgenic model mice. In brain homogenates with A β , the interaction of PrP^C and mGluR5 is reversed by mGluR5-directed antagonists or antibodies directed against PrP^C segment of aa 91-153. Silent allosteric modulators of mGluR5 do not alter Glu or basal mGluR5 activity, but they disrupt A β -induced interaction of mGluR5 with PrP^C. The assays described here have the potential to identify and develop new compounds that inhibit the interaction of PrP^C and mGluR5, which plays a pivotal role in the pathogenesis of Alzheimer's disease by transmitting the signal from extracellular A β into the cytosol.

Soluble amyloid- β oligomers (A β) are potent synaptotoxins and key mediators of Alzheimer disease (AD) pathophysiology (1-7). There is a robust correlation between disease severity and the

concentration of prefibrillar, soluble A β (8-10). In contrast, the load of insoluble fibrillar amyloid plaques correlates poorly with the degree of dementia (8,9,11-13). Recent progress in the field has improved our understanding of the mechanisms by which A β interact with synapses and trigger synaptotoxicity. Cellular prion protein (PrP^C) was identified as high-affinity cell-surface receptor for A β (14), which was confirmed both in vivo and in vitro (15-17). Numerous AD-related deficits are dependent on the presence of PrP^C, such as A β -triggered synaptic dysfunction, dendritic spine and synapse loss, serotonin axon degeneration, epileptiform discharges, spatial learning and memory impairment, and the reduced survival of APP/PS1 transgenic mice (1,14,18-22). A β -PrP^C complexes are extractable from human AD brains and human AD brain-derived A β inhibit synaptic function in a PrP^C-dependent manner (15,19,23,24). Furthermore, blockade of the interaction between A β and PrP^C, which was mapped to the regions 23-27 and 95-110 in PrP^C, prevents A β -induced inhibition of synaptic plasticity (14,17). However, the role of PrP^C as a mediator of A β -induced toxicity does not appear to apply for all A β conformers and all assay models. Both, Kessels et al. (2010) and Calella et al. (2010), found A β -induced impairment of hippocampal LTP independent of presence of PrP^C (25,26). Moreover, another study verified an A β -dependent decline of long-term memory consolidation that was independent of PrP^C (16). Variable outcomes in toxicity assays are most likely due to distinct compositions of different A β preparations. Several different isoforms of A β exist and certain forms have been demonstrated to trigger specific AD-related toxic effects, some of which might be independent of PrP^C (3,27-29). When A β /PrP^C-complexes form, they trigger AD pathophysiology by interacting with mGluR5 (30). Both PrP^C and mGluR5 receptors are located in lipid raft-like domains, and these are hypothesized to be the key location of A β -triggered induction of synaptotoxicity (31-34). Consistent with this finding, Renner et al. (2010) revealed a PrP^C- and mGluR5-dependent binding of A β to synapses using live single particle tracking of labeled A β in hippocampal neurons. They claim that A β cause synaptic dysfunction by triggering an abnormal clustering and overstabilization of mGluR5 receptors within the plasma membrane

(35). Moreover, mGluR5 receptors are implicated in excitotoxicity and in transducing signals from the cell-surface receptor PrP^C into the cytosol (36,37). Participation of mGluR5 in AD-disease related synaptotoxicity is consistent with the observation that A β -induced suppression of long-term potentiation (LTP) and enhancement of long-term depression (LTD) can be imitated by mGluR5 agonists and suppressed by mGluR5 antagonists (1,38-40). Furthermore, incubation of neurons with A β initiates secondary messenger cascades that mimic the activation of mGluR receptors (7). Thus, it is not surprising that multiple A β -induced AD-related deficits are dependent on the presence of both PrP^C and mGluR5. Some examples include A β -triggered reduction of LTP and enhancement of LTD, activation of intracellular Fyn kinase, A β -induced dendritic spine loss, and spatial learning and memory deficits of APP/PS1 transgenic mice (19,30,41,42). Assuming that the physical interaction of PrP^C with mGluR5 is essential for the transmission of A β -induced neurotoxic signals to intracellular substrates, targeting the PrP^C-mGluR5 interaction has potential clinical implications for AD. Development of therapeutic strategies would benefit from a more precise knowledge about the interaction between PrP^C and mGluR5. The structure of both PrP^C and mGluR5 have been characterized (43-45), potentially facilitating the study of their interaction and regulation by A β . In this study, we used a library of PrP^C deletion mutants as well as antibody mapping experiments to identify the region 91-153 of PrP^C as accounting for the interaction with mGluR5. Moreover, we provide evidence that the interaction of mGluR5 with PrP^C can be manipulated by agonist/antagonist-induced conformational changes of mGluR5 or antibody-blockade of PrP^C. Our findings also reveal a significant enhanced interaction between PrP^C and mGluR5 in the brain of mice expressing familial AD transgenes. This stimulatory effect of the APP transgene is mimicked by the artificial supply of A β and inhibited by both mGluR5-directed antagonists and PrP^C-directed antibodies, which target the binding sites of A β and mGluR5 on PrP^C.

EXPERIMENTAL PROCEDURES

A β 42 oligomer preparation

A β 42 oligomers were prepared as described

previously (14). All concentrations are given in monomer equivalents, with 1 μ M of total A β 42 peptide corresponding to approximately 10 nM oligomeric species (Lauren et al., 2009). A β was prepared immediately before use in glutamate-free F12 medium to avoid direct stimulation of glutamate receptors.

Mouse strains

All mouse strains have been described previously (18,46,47). Males and females were used in approximately equal numbers, and none were excluded.

Drugs and antibodies

The following metabotropic glutamate receptor-directed compounds were used:

ADX-47273 (S-(4-fluoro-phenyl)-{3-[3-(4-fluoro-phenyl)-[1,2,4]-oxadi-azol-5-yl]-piperidin-1-yl}-methanone, Selleckchem), DCB (3,3'-dichlorobenzaldazine, Tocris bioscience), 3,5-DHPG (Dihydroxyphenylglycine, Tocris bio-science), LY-456236 hydrochloride (6-Methoxy-N-(4-methoxyphenyl)-4-quinazolin-amine-hydrochloride, Tocris bioscience), MTEP hydrochloride (3-((2-Methyl-4-thiazolyl)ethynyl)pyridine, Tocris bioscience), SIB 1757 (6-methyl-2-(phenylazo)pyridin-3-ol, Tocris bioscience), VU-0357121 (4-Butoxy-N-(2,4-difluorophenyl)benzamide, Tocris bioscience). The following antibodies were used: 6D11 (mouse monoclonal, epitope between residues 97 and 100 of PrP^C, Covance/Signet), M-20 (affinity-purified goat polyclonal, raised against C-terminal part of mouse PrP^C, Santa Cruz Biotechnology). The following antibodies were used for antibody mapping experiments: 6D11 (Covance, epitope between residues 97 and 100), 3F4 (Covance, epitope between residues 108 and 111), Pri308 (Cayman Chemical, epitope between residues 106 and 126), 6G3 (Santa Cruz Biotechnology, epitope between residues 130 and 150), Bar 233 (Cayman Chemical, epitope between residues 141 and 151), Bar221 (Cayman Chemical, epitope between residues 141 and 151), M-20 (Santa Cruz Biotechnology, raised against C-terminal part of mouse PrP^C), 11C6 (Cayman Chemical, epitope between residues 142 and 160), SAF70 (Cayman Chemical, epitope between residues 156 and 162).

Cell culture and preparation of cell lysates

HEK-293T cells were maintained in Dulbecco's Modified Eagle Medium (DMEM), supplied with 10% fetal calf serum (FCS), 1% L-glutamine (2 mM f.c.), 1% sodium pyruvate (1 mM f.c.) and 1%

penicillin/streptomycin (100 U/ml). Cells were transfected using Lipofectamine 2000 transfection reagent (Invitrogen). To prepare detergent solubilized cell lysates, cells were rinsed with ice-cold phosphate-buffered saline (PBS) and solubilized in Radio Immuno Precipitation Assay (RIPA) buffer containing 150 mM sodium chloride, 1.0% NP-40, 0.5% sodium deoxycholate, 0.1% SDS, 50 mM Tris, pH 7.4, 1 mM EDTA, complete protease inhibitor cocktail (Roche), and phosSTOP phosphatase inhibitor cocktail (Roche). The insoluble fraction was removed by centrifugation at 20,000 \times g and the supernatant was used for protein assays.

Cell surface biotinylation

Cells were rinsed three times in ice-cold PBS to remove primary amine-containing culture media and incubated in PBS containing 2 mM EZ-Link NHS-Biotin (Thermo Scientific) for 30 min at 4°C. Cells were rinsed three times in quenching buffer (100 mM glycine in PBS) to block any unreacted NHS-biotin. Proteins were extracted in RIPA lysis buffer, separated by SDS-PAGE and analyzed by immunoblotting.

Preparation of RIPA soluble extracts from brain tissue

Mouse forebrains were homogenized in three volumes ice-cold (w/v) 50 mM Tris-HCl, 150 mM NaCl, pH 7.4 (TBS), complete protease inhibitor cocktail (Roche), and phosSTOP phosphatase inhibitor cocktail (Roche) using a Teflon homogenizer. Homogenized brain extract was centrifuged at 100,000 \times g for 20 min at 4°C and the pellet was resuspended in RIPA buffer. The resuspension was centrifuged at 100,000 \times g for 20 min. The supernatant was used for protein assays.

Crude Membrane preparations

HEK-293 cells or mouse forebrains were homogenized in homogenization buffer (10 mM Tris-HCl, pH 7.4, 1 mM EDTA, 200 mM sucrose, complete protease inhibitor cocktail (Roche), phosSTOP phosphatase inhibitor cocktail (Roche)) and insoluble material was removed by centrifugation at 900 \times g for 10 min at 4°C. The supernatant was centrifuged at 110,000 \times g for 75 min at 4 °C and the membrane pellet was resuspended in solubilization buffer (10 mM Tris-HCl, pH 7.4, 1 mM EDTA, complete protease inhibitor cocktail (Roche), phosphatase inhibitor (Roche)) for 3 h to over night at 4°C. Proteins were extracted by 1.0% NP-40 for 1 h at 4°C and used for protein assays.

Immunoprecipitation

One microgram of capture antibody was incubated overnight at 4°C with 1 mg of detergent solubilized lysate protein with continuous mixing. The antibodies used were anti-Myc (Sigma-Aldrich, C3956) for anti-Myc immunoprecipitation and Saf32 (Cayman, 189720) for anti-PrP^C immunoprecipitation in all experiments except anti-PrP^C immunoprecipitation experiments of PrP^C deletion mutants, where a mixture of both, Bar 233 (Cayman 10009036) and Saf32 (Cayman 189720), were used as capture antibodies. PureProteome Protein A/G Mix Magnetic Beads (Millipore, LSKMAGAG10) or Goat Anti-Rabbit IgG Magnetic Beads (New England BioLabs, S1432S) were washed in wash buffer (PBS + 0.1% Tween 20, pH 7.4), the preformed antibody-antigen complex added to the beads and incubated for 1 hour, in the case of HEK-293 cell experiments, or 3 hours, in the case of mouse brain experiments, at 4°C with gentle rotation. For some experiments, antibodies were covalently coupled to Protein A/G Mix Magnetic Beads. Here, beads were washed in wash buffer, incubated with double the amount of appropriate antibody for 1 hour at 4°C, and washed three times in wash buffer and once in crosslink buffer (20 mM sodium phosphate, 0.15 M NaCl, pH 7.4). Antibodies were then immobilized on the beads by incubation with 2.5 mM Bis(sulfosuccinimidyl) suberate (BS3) crosslinker for 1 hour at 4°C. The reaction was quenched by 17 mM Tris-HCl, pH 7.4 and incubation for 1 hour at 4°C. Not-immobilized antibodies were removed by one wash in 0.2 M Glycine-HCl, pH 2.5, followed by three washes in wash buffer. Beads were incubated with detergent-solubilized lysate overnight at 4°C with gentle rotation and washed three times in wash buffer prior to elution of proteins in SDS-PAGE sample loading buffer. The immunoprecipitated complexes were then resolved by SDS-PAGE and immunoblotted.

Plate-based binding assay of PrP^C-mGluR5

384-well white MaxiSorp microplates (Nunc, 460372) were coated with 20 µl/well of 150 µM purified recombinant PrP^C (AA23-230) overnight at 4°C. Plates were washed and blocked with 110 µl/well of protein-free PBS-T20 blocking buffer (Pierce) for 3-5 hours at RT. Immobilized PrP^C was exposed to detergent lysates of HEK-293 cells expressing Myc-mGluR (1% N-Nonanoyl-N-methylglucamine in PBS, complete protease

inhibitor cocktail (Roche), and phosphatase inhibitor (Roche)) in 3-fold serial dilutions and incubated over night at 4°C. Plates were washed and incubated with 20 µl/well of primary antibody solution (anti-Myc, 1:2,000 dilution in PBS-T) for 2 hours at room temperature. Plates were washed and incubated with 20 µl/well of secondary antibody solution (Europium-conjugated, 1:8,000 in DELFIA assay buffer) for 1-2 hours at room temperature. Plates were washed, 20 µL/well of DELFIA enhancement solution was added and imaging was performed using the Victor 3V microplate reader (Perkin Elmer).

Immunoblots

Proteins were electrophoresed through precast 4-20% tris-glycine gels (Bio-Rad) and transferred to nitrocellulose membranes (Invitrogen) with an iBlot™ Gel Transfer Device (Invitrogen). Membranes were blocked (Blocking Buffer for Fluorescent Western Blotting, Rockland MB-070-010) for 1 h at RT and incubated overnight in primary antibodies. The following antibodies were used: 6D11 (Covance 39810-500; 1:1,000), 6E10 (Millipore MAB 1560; 1:1,000), anti-actin (Sigma-Aldrich A2066; 1:10,000), anti-Myc (Sigma-Aldrich C3956; 1:1,000), anti-mGluR5 (Millipore AB5675; 1:500), Bar 233 (Cayman 10009036; 1:200), Saf32 (Cayman 189720; 1:200) and IRDye Streptavidin 680 (Odyssey; 1:20,000). Secondary antibodies were applied for 1 h at RT (Odyssey donkey anti-mouse or donkey anti-rabbit IRDye 680 or 800) and proteins were visualized with a Licor Odyssey infrared imaging system. Quantification of band intensities was performed within a linear range of exposure.

RESULTS

Mapping the mGluR5-interacting Region in PrP^C

The mGluR5 binding regions in PrP^C were mapped using PrP^C deletion mutants (Fig. 1) and antibody mapping experiments (Fig. 2). All PrP^C deletion mutants expressed at similar levels in HEK-293 cells (Fig. 1A, bottom panel and Fig. 1 C, bottom panel). Trafficking defects for the mutants were excluded by cell surface biotinylation of living cells with the membrane-impermeable chemical EZ-Link NHS-Biotin. A comparable streptavidin signal was observed in anti-PrP^C immunoprecipitates of cells expressing deletion mutants and the full-length version of PrP^C (Fig. 1A, top panel). This indicates that deletions do not prevent PrP^C mutants from

reaching the plasma membrane, which is a requirement to evaluate their interaction with mGluR5. Then, evaluation of the interaction between Myc-mGluR5 and different versions of PrP^C was performed (Fig. 1C). We found that deletions spanning the residues 91-153 reduced the interaction of PrP^C with mGluR5. Most strikingly, we observed a reduction in the amount of PrP^C-d91-111 pulled down after Myc-mGluR5 immunoprecipitation (Fig. 1C, $23 \pm 11\%$, n=4, blue bar) and the complementary reduction of the Myc-mGluR5-signal in PrP^C-d91-111 immunoprecipitation (Fig. 1D, $16 \pm 8.6\%$, n=4, blue bar), both compared to the full length PrP^C. Similarly, deletion of the beta-sheet rich region in PrP^C decreased the PrP^C signal in anti-Myc immunoprecipitates (Fig. 1D, $40 \pm 16\%$, n=4, red bar). Moreover, deletion of helix 1 in PrP^C showed a reduction in the Myc-mGluR5-signal in PrP^C immunoprecipitation (Fig. 1D, $40 \pm 9.5\%$, n=4, yellow bar). These results indicate that the region spanning residues 91-153 is involved in binding Myc-mGluR5. The absence of a reduced co-immunoprecipitation signal with the PrP^C deletion mutants that lack elements outside of region 91-153 imply that regions other than 91-153 are not essential for the interaction with mGluR5.

To confirm these results, we took a different approach to map the regions of PrP^C interacting with mGluR5. Recombinant full-length PrP^C was used to coat MaxiSorp microplates, which were then incubated with detergent-soluble membrane fractions prepared from HEK-293 cells expressing Myc-mGluR (Fig. 2). A robust signal was detected with Myc-mGluR5 lysates (Fig. 2A, black dotted line). Even though Myc-mGluR8 expression was higher than Myc-mGluR5 (Fig. 2B), the closely related protein Myc-mGluR8 (Fig. 2A, red dotted line) and control cell lysates (Fig. 2A, green dotted line) produced no detectable signal in the plate-based binding assay of PrP^C-mGluR, demonstrating the specificity of this assay towards Myc-mGluR5. Using this assay, we screened a panel of anti-prion protein antibodies for their ability to disrupt the interaction between Myc-mGluR5 with immobilized PrP^C (Fig. 2C). Antibodies recognizing the 91-111 region of PrP^C (6D11, 3F4, Pri308) blocked the protein interaction in a dose dependent manner (Fig. 2D). In addition, antibodies recognizing the beta-sheet rich region and helix 1 of PrP^C (BAR233, 6G3, BAR221) showed a similar interaction inhibition

(Fig. 2E). In contrast, control antibodies not recognizing PrP^C (GAPDH), and antibodies recognizing domains of PrP^C outside of region 91-153 (SAF70, M20, 11C6 and others not shown) had no effect on the interaction (Fig. 2F). These data are consistent with the deletion mapping results indicating that region 91-153 of PrP^C mediate the interaction with mGluR5.

Regulation of the PrP^C-mGluR5 Interaction

We analyzed whether or not the interaction between PrP^C and Myc-mGluR5 can be regulated by agonist/antagonist driven conformational changes of mGluR5 (Fig. 3). Our results indicate that negative allosteric modulators weaken the interaction between PrP^C and Myc-mGluR5, and the strongest effect was seen with MTEP. This drug reduces the co-immunoprecipitation of PrP^C with mGluR5 (Fig. 3C, $33 \pm 5.2\%$, n=12) and also the complementary co-immunoprecipitation (Fig. 3D, $46 \pm 6.9\%$, n=10), comparing with the full interaction signal of untreated cells. We observed that this MTEP-triggered negative regulation of the PrP^C-mGluR5 co-immunoprecipitation is dose-dependent (Fig. 4). On the other hand, agonists and positive allosteric modulators increased the co-immunoprecipitation of PrP^C and Myc-mGluR5, and the strongest effect was seen by treating cells and detergent solubilized lysates with the functional glutamate analogue DHPG (Fig. 3C,D). In the presence of DHPG, the PrP^C-mGluR5 interaction increased (Fig. 3C, $260 \pm 24\%$, n=11) when mGluR5 was immunoprecipitated and in the same fashion, the complementary co-immunoprecipitation was increased (Fig. 3D, $263 \pm 20\%$, n=11), as compared to the amount of co-immunoprecipitation in untreated cells. DCB is a silent allosteric modulator of mGluR5, competing with MTEP but not inhibiting the receptor (48). Application of DCB alone did not alter the interaction between PrP^C and Myc-mGluR5 (Fig. 3B). However, incubation of cells with DCB 10 minutes prior to application of MTEP prevented the blocking of the PrP^C-Myc-mGluR5 interaction triggered by MTEP (Fig. 3B, last lane). These results indicate that treatment with DCB prevents the negative allosteric modulator MTEP from inducing conformational changes that could alter the interaction of PrP^C and Myc-mGluR5.

Confirmation of Drug Specificity with Chimeric mGluRs

To further determine the drug specificity of alterations produced on the co-immunoprecipitation of PrP^C and Myc-mGluR5, driven by agonist/antagonist induced conformational alterations of mGluR5, we investigated the effect of mGluR5-directed endogenous ligand and agonists/antagonists on the interaction between PrP^C and different Myc-mGluR chimeras (Fig. 5). As a control, we co-transfected PrP^C and Myc-mGluR8. The co-immunoprecipitation of these proteins was significantly lower in comparison to the co-immunoprecipitation signal of Myc-mGluR5 with PrP^C (Fig. 5C,D red bar vs. black bar, $p = 0.0006$ and $p = 0.0005$ by one-sample t-test, respectively). Moreover, both chimeric Myc-mGluR-N5/C8 and Myc-mGluR-N8/C5 proteins co-immunoprecipitate less effectively with PrP^C compared to Myc-mGluR5 (Fig. 5C,D green and purple bar vs. black bar). These chimeric proteins contain the extracellular domain of either Myc-mGluR5 or Myc-mGluR8 and the transmembrane spanning domain of the other metabotropic receptor, respectively (Fig. 5B). As seen before, PrP^C and Myc-mGluR5 co-immunoprecipitate more effectively in the presence of glutamate and DHPG, but less effectively in the presence of MTEP (Fig. 5E,F). In contrast, MTEP did not show any effect on the co-immunoprecipitation of PrP^C and Myc-mGluR-N5/C8 (Fig. 5G,H). Moreover, the PrP^C-Myc-mGluR-N8/C5 co-immunoprecipitation signal was not affected by DHPG (Fig. 5I,J). Thus, the highly specific mGluR5-directed drugs MTEP and DHPG failed to alter the interaction between PrP^C and Myc-mGluR when their implicated receptor binding element was missing. In contrast, glutamate effects are observable across all classes of mGluRs. These results provide further mechanistic support for the specificity of the mGluR5 conformational regulation of PrP^C association.

Conformational Regulation of mGluR5 requires Membrane Environment

To determine whether the modulation of the PrP^C-mGluR5 complex strength by mGluR5 conformational changes (agonist/antagonist binding) is dependent on the stability of the plasma membrane, we analyzed how this modulation is affected by administration of agonist/antagonist to different cellular and subcellular fractions (Fig. 6). PrP^C and Myc-mGluR5 co-immunoprecipitate less effectively when MTEP is applied constantly at all steps of

the immunoprecipitation process, first to the intact cells and later to the detergent solubilized lysates. Similarly, DHPG is more effective when the drug is applied at all steps of the immunoprecipitation process (cells and detergent solubilized lysates) (Fig. 6A). This effect is even stronger when membrane preparations of untreated cells expressing PrP^C and Myc-mGluR5 are subsequently incubated with MTEP and DHPG (Fig. 6B). Membrane fractions were prepared in the absence of SDS, which confirms that the co-immunoprecipitation of PrP^C with Myc-mGluR5 does not occur in aggregated protein complexes and is not dependent on non-native protein interactions induced by SDS. Moreover, the regulation of this protein-protein interaction by mGluR5-directed drugs is still observable in the absence of denaturing detergent. However, compound-induced modulation of the PrP^C-Myc-mGluR5 interaction is less effective when cells or detergent solubilized lysates alone are incubated with MTEP or DHPG (Fig. 6C,D), with the lowest modulation seen in the Myc-mGluR5 co-immunoprecipitation with PrP^C after treatment of detergent solubilized lysates only (Fig. 6D). These results indicate that agonist/antagonist-induced modulations of the PrP^C-Myc-mGluR5 interaction are strong only when mGluR5 receptors are treated in their native membrane-embedded conformation and drugs are present throughout a co-immunoprecipitation.

Conformational Regulation of Endogenous Brain PrP^C-mGluR5 Interaction

We further investigated whether or not agonist/antagonist driven conformational states of mGluR5 are also able to regulate the brain PrP^C-mGluR5 interaction (Fig. 7). We first determined that co-immunoprecipitation of brain PrP^C with mGluR5 requires both proteins and is absent in either single *Grm5*^{-/-} or *Prnp*^{-/-} knock out mouse brain. Treatment of detergent solubilized membrane fractions of WT brain, cleared by 100,000 x g centrifugation after the extraction of membrane proteins by NP-40, show no agonist/antagonist dependent regulation of the mGluR5 signal in anti-PrP^C immunoprecipitates, even though co-immunoprecipitation is strong (Fig. 7A). However, the mGluR5 signal in anti-PrP^C immunoprecipitates is significantly altered when membrane fractions of WT brains were treated with mGluR5 agonists/antagonists, followed by the extraction of proteins with NP-40

and removal of large particulate material at 20,000 x g (Fig. 7B). As seen in HEK membranes above, MTEP-induced changes in the mGluR5 conformation trigger a less effective mGluR5-PrP^C interaction (Fig. 7C, red bar), whereas DHPG-induced changes in the mGluR5 conformation cause mGluR5 to co-immunoprecipitate more efficiently with PrP^C (Fig. 7C, green bar). This effect is seen in the absence of SDS, which further verifies that a modulatory interaction between brain PrP^C and mGluR5 is not dependent on non-native protein interactions. However, even after drug treatment of membrane fractions, if smaller proteolipid complexes are removed by 100,000 x g ultracentrifugation in the presence of NP-40, then ligand regulation of the protein-protein association is lost. These experiments demonstrate that drug-induced conformational changes of mGluR5 can regulate the brain PrP^C-mGluR5 complex interaction in a certain array of proteins and membrane environment.

Conformational Regulation of mGluR5 by Endogenous Ligands

The immunoprecipitation assays described here can also be used to examine the effects of the endogenous ligands of PrP^C and mGluR5, A β and glutamate respectively, on the co-immunoprecipitation of PrP^C and mGluR5 interaction between them (Fig. 8). Both glutamate and A β enhance the co-immunoprecipitation of PrP^C in Myc-immunoprecipitates in a similar manner as the mGluR5-directed agonist DHPG (Fig. 8B, grey bar, 278 \pm 28%, n=7; blue bar, 214 \pm 34%, n=8; green bar, 260 \pm 24%, n=11, respectively). Similar effects were seen in the complementary PrP^C-immunoprecipitation (Fig. 8C, grey bar, 242 \pm 27%, n=7; blue bar, 218 \pm 31%, n=8; green bar, 263 \pm 20%, n=11, respectively). However, pre-incubation of cells with DHPG prior to A β did not further increase the co-immunoprecipitation signal of PrP^C and Myc-mGluR5 (Fig. 8B,C, yellow bar), indicating occlusive action of the glutamate analogue DHPG and the endogenous ligand A β . The co-immunoprecipitation of PrP^C with Myc-mGluR5 in cells pre-incubated with MTEP prior to A β was not different to the co-immunoprecipitation of these proteins in untreated cells (Fig. 8B,C, orange bar vs. black bar). Thus, A β lose their ability to promote the formation of the complex when mGluR5 is in an inhibited conformation. Taken together, our results indicate that the endogenous ligands glutamate and A β

enhance the interaction between PrP^C and Myc-mGluR5, and this increased interaction can be reversed by MTEP-induced conformational changes of Myc-mGluR5.

A β -dependent Regulation of the PrP^C-mGluR5 Interaction requires Intact Lipid Rafts

A β effects are proposed to occur in lipid raft-like domains, to which PrP^C and mGluR5 are known to localize (31-33). We show that disruption of lipid rafts by pre-treatment of PrP^C and Myc-mGluR5 co-expressing HEK293 cells with methyl- β -cyclodextrin (M β CD) prevented A β -induced alterations of the PrP^C-Myc-mGluR5 interaction (Fig. 9).

Reversal of the A β -triggered augmented PrP^C-mGluR5 Interaction

Since A β -triggered augmented PrP^C-mGluR5 interaction is a potential step in the process of neurodegeneration, blocking this event might have therapeutic significance. To test whether PrP^C-directed antibodies or mGluR5-directed drugs other than MTEP could prevent the A β -triggered augmentation of the PrP^C-Myc-mGluR5 interaction, we analyzed their effect prior to A β administration on the co-immunoprecipitation of PrP^C with Myc-mGluR5 in absence of SDS (Fig. 10). A β increase the PrP^C co-immunoprecipitation with Myc-mGluR5 in HEK-293 cells (Fig. 10B, 214 \pm 34%, n=8, black bar). We analyzed a series of known therapeutic molecules to evaluate their effect on the pathological increased interaction between PrP^C and Myc-GluR5 promoted by A β . First we show that in the absence of A β , only the application of MTEP reduced the normal interaction between PrP^C and Myc-mGluR5 significantly (Fig. 10B, 33 \pm 5.2%, n=12, red bar). Also, sole application of DCB, 6D11 and Bar221 triggered a slight, but not significant decline of the steady state interaction between PrP^C and Myc-mGluR5 (Fig. 10B, yellow, purple and blue bar, respectively). Note that 6D11 and Bar221 reduced association in the plate based format (Fig. 2D,E), suggesting that association may be more resistant to regulation when formed in the cell membrane. We then tested whether PrP^C-directed antibodies or mGluR5-directed drugs reverse the A β -induced increase on the co-immunoprecipitation of PrP^C with Myc-mGluR5. Our findings revealed that, not only the mGluR5-directed antagonist MTEP, but also the silent allosteric modulator DCB reversed the A β -triggered increase of the co-immunoprecipitation

of PrP^C and Myc-mGluR5 (Fig. 10C, red and yellow bar, respectively). Moreover, two antibodies binding within the 91-153 region of PrP^C, 6D11 and Bar221, reversed the increase in the PrP^C-mGluR5 interaction triggered by A β (Fig. 10C, purple and blue bar, respectively). In contrast, the antibody M20 binding outside of the 91-153 region of PrP^C, did not reverse the enhanced co-immunoprecipitation signal of PrP^C and mGluR5 triggered by A β (Fig. 10C, green bar). These experiments demonstrate that mGluR5-directed drugs and PrP^C-directed antibodies targeting the A β - and/or mGluR5-binding site on PrP^C, but not antibodies targeting regions outside of this binding site, can reverse the A β -induced stimulation of the PrP^C-mGluR5 interaction.

mGluR5 Conformational Regulation in Alzheimer Model Mouse Brain

We further analyzed whether an increase of the co-immunoprecipitation signal of PrP^C with mGluR5 is caused exclusively by an acute synthetic A β administration, or whether or not this effect can also be observed in transgenic AD mouse model brain due to endogenous A β *in vivo* (Fig. 11). We observed that the mGluR5 co-immunoprecipitation with PrP^C is increased 2.5-fold in APP/PS1⁺ transgenic brain compared with WT brain (Fig. 11C, red bar; Fig. 10D, 309 \pm 76%, grey bar; n=9). This is similar to treatment of WT brain-derived membrane fractions with exogenous A β . Here, A β enhanced the mGluR5 signal in PrP^C immunoprecipitates 1.9-fold, in comparison to untreated membrane fractions (Fig. 11D, 189 \pm 27%, green bar). To further elucidate whether or not a drug- or antibody-induced modulatory effect can reverse this A β -induced increase in the PrP^C-mGluR5 interaction, we prepared brain membrane fractions of WT and APP/PS1⁺ transgenic animals in absence of SDS and incubated these with either A β , mGluR5-directed compounds, PrP^C-directed antibody 6D11, or a combination of A β and therapeutic molecules. We observed that the A β -dependent increase in the co-immunoprecipitation signal was significantly reduced by MTEP (Fig. 11D, red bar). A trend for the reversal of the A β -triggered increase of the PrP^C-mGluR5 co-immunoprecipitation in WT brain membrane fractions by 6D11 was also observable (Fig. 11D, purple bar). Moreover, we found that incubation of APP/PS1⁺ transgenic brain-derived membrane fractions with either the mGluR5-directed

antagonist MTEP or the PrP^C-directed antibody 6D11 fully reversed the enhanced PrP^C-mGluR5 co-immunoprecipitation triggered by presence of the APP/PS1⁺ transgenic background (Fig. 11D, blue bar and orange bar, respectively). Application of the silent allosteric modulator DCB produced a trend to recover the increased interaction of PrP^C and mGluR5 in brain-derived membrane fractions of APP/PS1⁺ transgenic animals (Fig. 11D, yellow bar). These results imply a mechanism by which the APP/PS1⁺ background in AD transgenic mice or acute A β -administration enhance the interaction between brain PrP^C and mGluR5, which can be reversed by mGluR5-directed drugs or PrP^C-directed antibodies targeting the binding site of mGluR5 and A β on PrP^C.

DISCUSSION

This study provides important insights into the interaction between PrP^C and mGluR5, which has therapeutic significance for the treatment of AD. We determined the site of interaction between mGluR5 and PrP^C to be exclusively dependent on region 91-153 of PrP^C. Our report further demonstrates that pharmacological manipulation of the interaction between PrP^C and mGluR5 rescues A β -triggered AD-related phenotypes. These findings provide further evidence to support the role of both PrP^C and mGluR5 in A β -induced pathophysiology.

Significance of PrP^C and mGluR5 in AD-related Phenotypes

PrP^C is a high-affinity cell-surface receptor for A β and is involved in a number of AD-related phenotypes (14,15,18-23). Despite the consistent finding of A β binding to PrP^C, some conflicting reports exist concerning the role of PrP^C in A β -induced synaptotoxicity and memory consolidation (16,25,26). Kessels et al. (2010) found an A β -induced impairment of hippocampal LTP independent of genetic Prnp background (25). Also, Calella et al. (2010) observed an A β -triggered decrease of synaptic plasticity unaffected by ablation or overexpression of PrP^C (26). Moreover, Balducci et al. (2010) found A β -dependent reduced consolidation of the long-term recognition memory independent of PrP^C (16). These studies challenged the role of PrP^C as a mediator of A β -induced toxicity. However, the composition of A β preparations between different studies varies greatly and is likely to account for inconsistent outcomes of functional

A β -dependent experiments (24). This stresses the need for a thorough characterization of A β preparations prior to functional studies to prevent A β -induced nonspecific toxicity that is independent of cell-surface receptors like PrP^C.

Less is known about the events downstream of the A β -PrP^C complex, with a crucial element being the transmission from A β -PrP^C complexes onto intracellular targets. Electrophysiological studies regarding the synaptotoxic effects of A β provided the first strong evidence for a critical role of mGluR5 receptors in A β -triggered AD-related phenotypes. Several studies demonstrated the recovery of A β -induced inhibition of LTP by mGluR5-directed antagonists (1,38-40). Further support comes from a comparison of mGluR5 glutamate- and A β -triggered intracellular signaling. Glutamate binding to the extracellular region of mGluRs induces conformational changes, which triggers G-protein activation and intracellular responses (49,50). Activation of group I mGluRs, comprising mGluR1 and mGluR5, activates phospholipase C β 1 (PLC β 1) via G $_{\alpha q/11}$ proteins (51). This triggers hydrolysis of phosphatidylinositol-4,5-bisphosphate membrane phospholipids to inositol-1,4,5-trisphosphate and diacylglycerol, which causes the release of intracellular Ca²⁺ and activation of protein kinase C (PKC) (52,53). Interestingly, incubation of mature neurons with A β mimics the decline of the phosphatidylinositol-4,5-bisphosphate level and the increase of intracellular Ca²⁺ seen by activation of mGluR5 (7,19,30). Further evidence for these indications was provided by identification of mGluR5 as co-receptor for A β bound to PrP^C (54).

Mapping the mGluR5-interacting Regions in PrP^C
A β -PrP^C-binding to mGluR5 triggers some aspects of AD pathophysiology. Pharmacological strategies targeting the PrP^C-mGluR5 interaction would largely benefit from a better understanding of the interaction between PrP^C and mGluR5. Human PrP^C is a 209-residue glycoprotein, anchored into the membrane of lipid rafts by a glycosylphosphatidylinositol (GPI) anchor (32,55). It contains two potential glycosylation sites at residues N181 and N197, respectively. Region 23-111 of PrP^C is intrinsically unstructured, preceded by a 22-residue long signal peptide. The intrinsically unstructured part of PrP^C is subdivided into the so-called octarepeat region (residues 60-91), a charged cluster (residues 91-

111), and a hydrophobic, beta-sheet containing region (residues 112-134). The C-terminal domain of PrP^C is mainly α -helical, harboring three individual α -helices. Helix 2 and helix 3 are connected by a disulphide bond between residues C179 and C214, respectively (43).

Here, we demonstrate that aa 91-153 of PrP^C mediate mGluR5 binding. Our findings are based on co-immunoprecipitation experiments of PrP^C-deletion mutants and mGluR5. These experiments revealed that PrP^C's region 91-111 is necessary for mGluR5-binding. Our results further implicate that the adjacent structural elements, the beta-sheet rich region and helix 1, are also involved in mGluR5-binding. We hypothesize that the entire region 91-153 mediates the binding to mGluR5, or, that deletion of beta-sheet rich region/helix 1 triggers conformational changes in region 91-111 that inhibits the interaction of PrP^C-dBeta or PrP^C-dHelix-1 with mGluR5. These results were further verified in an anti-prion protein antibody screen. Antibodies directed against region 91-111, beta-sheet rich region or helix 1 of PrP^C largely reduced the Myc-mGluR5 binding to immobilized PrP^C. In contrast, deletion of structural elements outside of region 91-153 or antibodies recognizing domains of PrP^C other than region 91-153 had no effect on the PrP^C-mGluR5 interaction.

Mapping the PrP^C-interacting Regions in mGluR5
The mGluR structure is composed of an extracellular region, a seven transmembrane-spanning region and a cytoplasmic region (44,45,56). To determine the region in mGluR5 accounting for interaction with PrP^C, we used chimeric proteins composed of the extracellular region of either Myc-mGluR5 or Myc-mGluR8 and the transmembrane spanning region of the other receptor in co-immunoprecipitation experiments with PrP^C. As a control, we co-transfected the closely related Myc-mGluR8 receptor and PrP^C. The co-immunoprecipitation of these proteins was significantly reduced in comparison to the co-immunoprecipitation signal of Myc-mGluR5 with PrP^C. Both chimeric Myc-mGluR-N5/C8 and Myc-mGluR-N8/C5 proteins revealed intermediate levels of binding to PrP^C. We observed a similar trend before (30), which indicates that the PrP^C-interacting regions are spread throughout the protein rather than being localized in either the extracellular or the transmembrane spanning mGluR region alone.

Pharmacological Manipulation of the PrP^C-mGluR5 Interaction

mGluR5 is implicated in a number of neurological diseases including Fragile X, Amyotrophic Lateral Sclerosis, Multiple Sclerosis, AD, Parkinson's disease, Huntington's disease, Epilepsy, Schizophrenia, and drug addiction, and its pharmacological tangibility is extensively studied (51,57-62). Moreover, anti-prion protein therapeutics were developed as putative treatments for prion disease (reviewed in Trevitt & Collinge (2006):(63)) and are available for screening their efficiency in regulating the PrP^C-mGluR5 interaction. Since the PrP^C-mGluR5 interaction is implicated in AD pathogenesis, we decided to develop assays to study the modulatory effect of therapeutic molecules on the interaction between mGluR5 and PrP^C. Our results demonstrated that agonist/antagonist-induced conformational changes of mGluR5 and PrP^C-directed antibodies alter the interaction between PrP^C and mGluR5 in a dose-dependent manner, both in HEK-293 cells and mouse brains.

Alternatives to Negative Allosteric Modulators

Our findings demonstrate a strong inhibitory effect of negative allosteric modulators, such as MTEP, on the PrP^C-mGluR5 interaction. However, mGluR5 function is important for healthy brain aging and intervention should, therefore, be aimed at regulating the PrP^C-mGluR5 interaction without modifying its physiological function in a negative way (53,64). mGluR5-directed antagonists inhibit glutamate signaling thereby negatively affecting normal cell signaling. A better pharmacological strategy for disease intervention is the use of so-called silent allosteric modulators. These do not affect glutamate signaling and therefore reduce possible side effects. However they alter the conformation of metabotropic glutamate receptors and prevent the action of e.g. other allosteric modulators (48). Our results show that application of the silent allosteric modulator DCB did not alter the PrP^C-mGluR5 interaction in the absence of A β o. However, pre-incubation of cells with DCB prior to application of the negative allosteric modulator MTEP blocks an inhibitory effect of MTEP on the PrP^C-Myc-mGluR5 interaction. Our findings are consistent with DCB occupancy preventing MTEP from binding to mGluR5 (48), which explains the lack of effect on the co-immunoprecipitation signal of PrP^C with Myc-

mGluR5 in untreated cells in comparison to DCB and MTEP double treated cells.

Confirmation of Drug Specificity with Chimeric mGluRs

To provide further mechanistic support for the specificity of the here-developed assays, we tested the effect of mGluR5-directed compounds on the interaction of PrP^C with either Myc-mGluR5, Myc-mGluR-N5/C8, Myc-mGluR-N8/C5 or Myc-mGluR8 as negative control. The co-immunoprecipitation signal of PrP^C with Myc-mGluR5 was regulated by glutamate, DHPG and MTEP, as seen before. However, MTEP did not regulate the co-immuno-precipitation of PrP^C with Myc-mGluR-N5/C8. Also, DHPG failed to modulate the co-immunoprecipitation of PrP^C and Myc-mGluR-N8/C5. These findings provide evidence for the drug specificity in the here-developed assays since the Myc-mGluR-N5/C8 mutant protein does not contain the transmembrane spanning part of mGluR5, which is targeted by MTEP (61). DHPG, on the other hand, is highly specific for the extracellular binding pocket of metabotropic group 1 receptors, which includes mGluR5 but not mGluR8 (61,65).

Conformational Regulation of mGluR5 requires Membrane Environment

We found that a modulatory effect on the interaction between PrP^C and mGluR5 is only observable when mGluR5 receptors are manipulated in their membrane-embedded conformation. Extraction of receptors from the lipid bilayer hinders agonist/antagonist-triggered conformational changes of mGluR5, which prevents an alteration of its interaction with PrP^C. However, our findings also show a less efficient modulation of the mGluR5-PrP^C interaction after agonist/antagonist treatment of cells only, in comparison to the treatment of membrane preparations or both, cells and detergent solubilized lysates. This effect is most likely due to a washout of compounds during the harvest and lysis of cells, as well as during the time-consuming immunoprecipitation.

Moreover, we failed to modulate the PrP^C-mGluR5 interaction in brain-derived membrane fractions cleared by 100,000 x g centrifugation after the extraction of membrane proteins. In contrast, conformational regulation of the mGluR5-PrP^C co-immunoprecipitation was observable when extracted proteins were cleared by 20,000 x g centrifugation removal. These

findings suggest that small proteolipid complexes contain PrP^C and mGluR5 in a pharmacologically vulnerable conformation. A 100,000 x g centrifugation removes those complexes needed to observe a compound-induced modulatory effect on the PrP^C-mGluR5 interaction. Taken together, a conformational change can only occur if mGluR5 is in its native lipid-associated conformation and environment. A conformational change can only trigger a modulation of the co-immunoprecipitation signal of Myc-mGluR5 and PrP^C if the same compound concentration is supplied throughout all steps of co-immunoprecipitation to prevent a washout of compounds, and if complexes are not removed by 100,000 x g centrifugation after detergent addition.

Similarities between mGluR5 Agonist-induced Conformational Changes and the Effect of A β

We further report that soluble A β consistently induced an enhancement of the PrP^C-mGluR5 co-immunoprecipitation, both in HEK-293 cell and mouse brain. Pre-incubation of HEK-293 cells with mGluR5-directed agonist DHPG prior to A β application did not further stimulate the PrP^C-mGluR5 signal. This indicates an occlusive action of DHPG and A β . One possible explanation is an overlapping binding site of A β -PrP^C complexes and DHPG on mGluR5, the latter of which is located in the extracellular binding pocket (61,65). The effect could also be explained by DHPG-triggered conformational changes of mGluR5, which prevents A β -PrP^C complexes from binding and inducing further conformational alterations. Our previous results showed that exclusive application of A β or DHPG trigger eEF2 phosphorylation in neurons (30). Application of both, A β and DHPG, did not further increase eEF2 phosphorylation, which is in accordance with the findings of HEK-293 cell experiments highlighted here. We further demonstrated that the A β -dependent enhancement of the PrP^C-mGluR5 interaction is dependent on the existence of lipid raft like domains. Pre-treatment of PrP^C and Myc-mGluR5 expressing cell cultures with M β CD destroyed lipid rafts and prevented an A β -dependent modulation of the PrP^C-Myc-mGluR5 interaction. This is in accordance with the fact that A β effects are proposed to occur in lipid raft like domains, where PrP^C and mGluR5 receptors are located (31-34).

mGluR5 Conformational Regulation in Alzheimer Model Mouse Brain

Furthermore, we provide evidence for a strongly enhanced mGluR5 signal in anti-PrP^C immunoprecipitates of APP/PS1⁺ transgenic mouse brain. These findings strongly support the potential value of therapeutically targeting the PrP^C-mGluR5 interaction in AD pathogenesis. The effect of the APP/PS1⁺ transgene or artificial supply of A β was rescued by the mGluR5-directed antagonist MTEP. MTEP induces a strong conformational change of mGluR5, which reverses the A β -induced enhanced interaction of PrP^C with mGluR5. This is of high biological relevance due to findings of previous studies that demonstrated the reversal of A β -induced effects in cell based toxicity assays by the mGluR5-specific antagonist MTEP (19,30). Moreover, MTEP treatment rescues AD-related learning and memory deficits in APP/PS1⁺ transgenic mice, which is in accordance with the here-described MTEP-induced reversal of AD-related molecular phenotypes (30). However, more feasible therapeutic agents for AD are silent allosteric modulators that do not affect endogenous glutamate signaling. In our experiments, the silent allosteric modulator DCB fully rescued A β -induced association in transfected cell lysates, and partially rescued the APP/PS1⁺ transgene-dependent enhancement of the PrP^C-mGluR5 interaction. Moreover, application of antibodies directed against the putative PrP^C-mGluR5 binding site (6D11, Bar233) or the A β -PrP^C binding site (6D11) prohibited the acute A β -induced or APP/PS1⁺ transgene-dependent augmentation of the PrP^C-mGluR5 co-immunoprecipitation. In contrast, M20, a polyclonal antibody targeting the C-terminal region of PrP^C, did not significantly alter A β -triggered changes in the PrP^C-mGluR5 co-immunoprecipitation. These findings are in line with the mapping of mGluR5-interacting regions in PrP^C to residues 91-153. Notably, exclusive application of 6D11 and Bar 221 did not reveal a strong effect on the co-immunoprecipitation of PrP^C and Myc-mGluR5. In contrast, 6D11 and Bar 221 showed a robust blockade of the Myc-mGluR5 binding to immobilized recombinant PrP^C in antibody mapping experiments of the binding site of Myc-mGluR5 on PrP^C. This indicates that the PrP^C-directed antibodies 6D11 and Bar 221 cannot easily access PrP^C interacting with mGluR5. In contrast, 6D11 and Bar 221 antibody binding to immobilized recombinant PrP^C blocks further binding of Myc-mGluR5. Interestingly, co-

incubation of membrane fractions of PrP^C and Myc-mGluR5 expressing HEK-293 cells with A β and PrP^C-directed antibodies 6D11 and Bar 221 altered the PrP^C-mGluR5 interaction to a larger extent than exclusive application of PrP^C-directed antibodies. These findings indicate that A β trigger a conformational change of the PrP^C-Myc-mGluR5 complex that renders PrP^C more vulnerable to antibody treatment by enabling the binding of anti-prion protein antibodies.

The Putative Role of mGluR5 in AD

We hypothesize that mGluR5 plays a crucial role in Alzheimer's disease pathogenesis by transmitting neurotoxic signals from extracellular A β -PrP^C complexes into the cytosol. Beraldo et al. (2011) report that binding of laminin to PrP^C alters neuronal plasticity and memory by mGluR1/5 mediated transmission of signals into the cytosol (36). Similar events are likely to occur after binding of A β to PrP^C, such as mGluR5-mediated transmission of signals onto intracellular substrates. Different substrates are feasible, one of which is Fyn kinase, whose activation provides a link to the NR2B subunit phosphorylation and redistribution of NMDA receptors observed after acute A β treatment (19,30,42). NMDA receptors are involved in LTP and their significance for AD is stressed by the symptomatic benefits of pharmacological NMDA receptor antagonists like Memantine (66,67). One possibility to explain the A β -PrP^C-induced signal transmission mediated by mGluR5 is the redistribution and overstabilization of mGluR5 receptors after A β -PrP^C binding, as seen by Renner et al. (2010) (35). mGluR5 receptors are normally laterally mobile within the membrane (68). It is feasible that A β -PrP^C complexes act like an extracellular scaffold stabilizing mGluR5, thereby preventing their lateral diffusion. A reduced diffusion efficiency of mGluR5 causes disruptive Ca²⁺ signaling, which alters NMDA receptor activity (69). Preventing A β -PrP^C complexes from binding to mGluR5 could ameliorate these putative neurotoxic events.

Future Directions

The assays described here can be used to identify therapeutic molecules that inhibit the interaction between PrP^C and mGluR5, whose signaling is implicated in AD pathogenesis. Whether prohibiting the binding of PrP^C to mGluR5 will eventually reduce neuronal loss and memory deficits in AD still needs to be determined. Moreover, activation of mGluR5 receptors is

known to stimulate several signaling pathways, some of which are involved in cell survival and proliferation, such as the extracellular signal-regulated kinase (ERK) and AKT pathway (70,71). Future research is necessary to determine the role of A β -PrP^C-mGluR5 complexes in these pathways. mGluR5 receptors are also known to be part of large multimolecular complexes (72). Further studies could determine additional modulators of the A β -PrP^C-mGluR5 interaction and such factors could potentially have tangibility for AD therapeutic research. Despite extensive research in the field, a preventive or disease modifying treatment for AD is still not available, generating one of the biggest threats to public health of this century. This stresses the need to find and characterize novel pharmacological targets for AD therapeutic intervention.

REFERENCES

1. Shankar, G. M., Li, S., Mehta, T. H., Garcia-Munoz, A., Shepardson, N. E., Smith, I., Brett, F. M., Farrell, M. A., Rowan, M. J., Lemere, C. A., Regan, C. M., Walsh, D. M., Sabatini, B. L., and Selkoe, D. J. (2008) Amyloid-beta protein dimers isolated directly from Alzheimer's brains impair synaptic plasticity and memory. *Nat Med* **14**, 837-842
2. Walsh, D. M., Klyubin, I., Fadeeva, J. V., Cullen, W. K., Anwyl, R., Wolfe, M. S., Rowan, M. J., and Selkoe, D. J. (2002) Naturally secreted oligomers of amyloid beta protein potently inhibit hippocampal long-term potentiation in vivo. *Nature* **416**, 535-539
3. Lesne, S., Koh, M. T., Kotilinek, L., Kaye, R., Glabe, C. G., Yang, A., Gallagher, M., and Ashe, K. H. (2006) A specific amyloid-beta protein assembly in the brain impairs memory. *Nature* **440**, 352-357
4. Lambert, M. P., Barlow, A. K., Chromy, B. A., Edwards, C., Freed, R., Liosatos, M., Morgan, T. E., Rozovsky, I., Trommer, B., Viola, K. L., Wals, P., Zhang, C., Finch, C. E., Krafft, G. A., and Klein, W. L. (1998) Diffusible, nonfibrillar ligands derived from Abeta1-42 are potent central nervous system neurotoxins. *Proc Natl Acad Sci U S A* **95**, 6448-6453
5. Li, S., Hong, S., Shepardson, N. E., Walsh, D. M., Shankar, G. M., and Selkoe, D. (2009) Soluble oligomers of amyloid Beta protein facilitate hippocampal long-term depression by disrupting neuronal glutamate uptake. *Neuron* **62**, 788-801
6. Palop, J. J., and Mucke, L. (2010) Amyloid-beta-induced neuronal dysfunction in Alzheimer's disease: from synapses toward neural networks. *Nat Neurosci* **13**, 812-818
7. Berman, D. E., Dall'Armi, C., Voronov, S. V., McIntire, L. B., Zhang, H., Moore, A. Z., Staniszewski, A., Arancio, O., Kim, T. W., and Di Paolo, G. (2008) Oligomeric amyloid-beta peptide disrupts phosphatidylinositol-4,5-bisphosphate metabolism. *Nat Neurosci* **11**, 547-554
8. Lue, L. F., Kuo, Y. M., Roher, A. E., Brachova, L., Shen, Y., Sue, L., Beach, T., Kurth, J. H., Rydel, R. E., and Rogers, J. (1999) Soluble amyloid beta peptide concentration as a predictor of synaptic change in Alzheimer's disease. *Am J Pathol* **155**, 853-862
9. McLean, C. A., Cherny, R. A., Fraser, F. W., Fuller, S. J., Smith, M. J., Beyreuther, K., Bush, A. I., and Masters, C. L. (1999) Soluble pool of Abeta amyloid as a determinant of severity of neurodegeneration in Alzheimer's disease. *Ann Neurol* **46**, 860-866
10. Wang, J., Dickson, D. W., Trojanowski, J. Q., and Lee, V. M. (1999) The levels of soluble versus insoluble brain Abeta distinguish Alzheimer's disease from normal and pathologic aging. *Exp Neurol* **158**, 328-337
11. Terry, R. D., Masliah, E., Salmon, D. P., Butters, N., DeTeresa, R., Hill, R., Hansen, L. A., and Katzman, R. (1991) Physical basis of cognitive alterations in Alzheimer's disease: synapse loss is the major correlate of cognitive impairment. *Ann Neurol* **30**, 572-580
12. Katzman, R., Terry, R., DeTeresa, R., Brown, T., Davies, P., Fuld, P., Renbing, X., and Peck, A. (1988) Clinical, pathological, and neurochemical changes in dementia: a subgroup with preserved mental status and numerous neocortical plaques. *Ann Neurol* **23**, 138-144
13. Dickson, D. W., Crystal, H. A., Bevona, C., Honer, W., Vincent, I., and Davies, P. (1995) Correlations of synaptic and pathological markers with cognition of the elderly. *Neurobiol Aging* **16**, 285-298; discussion 298-304
14. Lauren, J., Gimbel, D. A., Nygaard, H. B., Gilbert, J. W., and Strittmatter, S. M. (2009) Cellular prion protein mediates impairment of synaptic plasticity by amyloid-beta oligomers. *Nature* **457**, 1128-1132
15. Zou, W. Q., Xiao, X., Yuan, J., Puoti, G., Fujioka, H., Wang, X., Richardson, S., Zhou, X., Zou, R., Li, S., Zhu, X., McGeer, P. L., McGeehan, J., Kneale, G., Rincon-Limas, D. E., Fernandez-Funez, P., Lee, H. G., Smith, M. A., Petersen, R. B., and Guo, J. P. (2011) Amyloid-beta42 interacts mainly with insoluble prion protein in the Alzheimer brain. *J Biol Chem* **286**, 15095-15105
16. Balducci, C., Beeg, M., Stravalaci, M., Bastone, A., Scip, A., Biasini, E., Tapella, L., Colombo, L., Manzoni, C., Borsello, T., Chiesa, R., Gobbi, M., Salmona, M., and Forloni, G. (2010) Synthetic amyloid-beta oligomers impair long-term memory independently of cellular prion protein. *Proceedings of the National Academy of Sciences of the United States of America* **107**, 2295-2300

17. Chen, S., Yadav, S. P., and Surewicz, W. K. (2010) Interaction between human prion protein and amyloid-beta (A β) oligomers: role OF N-terminal residues. *The Journal of biological chemistry* **285**, 26377-26383
18. Gimbel, D. A., Nygaard, H. B., Coffey, E. E., Gunther, E. C., Lauren, J., Gimbel, Z. A., and Strittmatter, S. M. (2010) Memory impairment in transgenic Alzheimer mice requires cellular prion protein. *J Neurosci* **30**, 6367-6374
19. Um, J. W., Nygaard, H. B., Heiss, J. K., Kostylev, M. A., Stagi, M., Vortmeyer, A., Wisniewski, T., Gunther, E. C., and Strittmatter, S. M. (2012) Alzheimer amyloid-beta oligomer bound to postsynaptic prion protein activates Fyn to impair neurons. *Nature neuroscience* **15**, 1227-1235
20. Bate, C., and Williams, A. (2011) Amyloid-beta-induced synapse damage is mediated via cross-linkage of cellular prion proteins. *J Biol Chem* **286**, 37955-37963
21. Kudo, W., Lee, H. P., Zou, W. Q., Wang, X., Perry, G., Zhu, X., Smith, M. A., Petersen, R. B., and Lee, H. G. (2012) Cellular prion protein is essential for oligomeric amyloid-beta-induced neuronal cell death. *Human molecular genetics* **21**, 1138-1144
22. Chung, E., Ji, Y., Sun, Y., Kascsak, R. J., Kascsak, R. B., Mehta, P. D., Strittmatter, S. M., and Wisniewski, T. (2010) Anti-PrPC monoclonal antibody infusion as a novel treatment for cognitive deficits in an Alzheimer's disease model mouse. *BMC Neurosci* **11**, 130
23. Barry, A. E., Klyubin, I., Mc Donald, J. M., Mably, A. J., Farrell, M. A., Scott, M., Walsh, D. M., and Rowan, M. J. (2011) Alzheimer's disease brain-derived amyloid-beta-mediated inhibition of LTP in vivo is prevented by immunotargeting cellular prion protein. *The Journal of neuroscience : the official journal of the Society for Neuroscience* **31**, 7259-7263
24. Freir, D. B., Nicoll, A. J., Klyubin, I., Panico, S., Mc Donald, J. M., Risse, E., Asante, E. A., Farrow, M. A., Sessions, R. B., Saibil, H. R., Clarke, A. R., Rowan, M. J., Walsh, D. M., and Collinge, J. (2011) Interaction between prion protein and toxic amyloid beta assemblies can be therapeutically targeted at multiple sites. *Nat Commun* **2**, 336
25. Kessels, H. W., Nguyen, L. N., Nabavi, S., and Malinow, R. (2010) The prion protein as a receptor for amyloid-beta. *Nature* **466**, E3-4; discussion E4-5
26. Calella, A. M., Farinelli, M., Nuvolone, M., Mirante, O., Moos, R., Falsig, J., Mansuy, I. M., and Aguzzi, A. (2010) Prion protein and A β -related synaptic toxicity impairment. *EMBO Mol Med* **2**, 306-314
27. Gandy, S., Simon, A. J., Steele, J. W., Lublin, A. L., Lah, J. J., Walker, L. C., Levey, A. I., Krafft, G. A., Levy, E., Checler, F., Glabe, C., Bilker, W. B., Abel, T., Schmeidler, J., and Ehrlich, M. E. (2010) Days to criterion as an indicator of toxicity associated with human Alzheimer amyloid-beta oligomers. *Annals of neurology* **68**, 220-230
28. Reed, M. N., Hofmeister, J. J., Jungbauer, L., Welzel, A. T., Yu, C., Sherman, M. A., Lesne, S., LaDu, M. J., Walsh, D. M., Ashe, K. H., and Cleary, J. P. (2011) Cognitive effects of cell-derived and synthetically derived A β oligomers. *Neurobiology of aging* **32**, 1784-1794
29. Cheng, I. H., Scarce-Levie, K., Legleiter, J., Palop, J. J., Gerstein, H., Bien-Ly, N., Puolivali, J., Lesne, S., Ashe, K. H., Muchowski, P. J., and Mucke, L. (2007) Accelerating amyloid-beta fibrillization reduces oligomer levels and functional deficits in Alzheimer disease mouse models. *J Biol Chem* **282**, 23818-23828
30. Um, J. W., Kaufman, A. C., Kostylev, M., Heiss, J. K., Stagi, M., Takahashi, H., Kerrisk, M. E., Vortmeyer, A., Wisniewski, T., Koleske, A. J., Gunther, E. C., Nygaard, H. B., and Strittmatter, S. M. (2013) Metabotropic glutamate receptor 5 is a coreceptor for Alzheimer abeta oligomer bound to cellular prion protein. *Neuron* **79**, 887-902
31. Francesconi, A., Kumari, R., and Zukin, R. S. (2009) Regulation of group I metabotropic glutamate receptor trafficking and signaling by the caveolar/lipid raft pathway. *J Neurosci* **29**, 3590-3602
32. Agostini, F., Dotti, C. G., Perez-Canamas, A., Ledesma, M. D., Benetti, F., and Legname, G. (2013) Prion protein accumulation in lipid rafts of mouse aging brain. *PLoS ONE* **8**, e74244
33. Zampagni, M., Evangelisti, E., Cascella, R., Liguri, G., Becatti, M., Pensalfini, A., Uberti, D., Cenini, G., Memo, M., Bagnoli, S., Nacmias, B., Sorbi, S., and Cecchi, C. (2010) Lipid rafts are primary mediators of amyloid oxidative attack on plasma membrane. *J Mol Med (Berl)* **88**, 597-608

34. Rushworth, J. V., Griffiths, H. H., Watt, N. T., and Hooper, N. M. (2013) Prion protein-mediated toxicity of amyloid-beta oligomers requires lipid rafts and the transmembrane LRP1. *The Journal of biological chemistry* **288**, 8935-8951
35. Renner, M., Lacor, P. N., Velasco, P. T., Xu, J., Contractor, A., Klein, W. L., and Triller, A. (2010) Deleterious effects of amyloid beta oligomers acting as an extracellular scaffold for mGluR5. *Neuron* **66**, 739-754
36. Beraldo, F. H., Arantes, C. P., Santos, T. G., Machado, C. F., Roffe, M., Hajj, G. N., Lee, K. S., Magalhaes, A. C., Caetano, F. A., Mancini, G. L., Lopes, M. H., Americo, T. A., Magdesian, M. H., Ferguson, S. S., Linden, R., Prado, M. A., and Martins, V. R. (2011) Metabotropic glutamate receptors transduce signals for neurite outgrowth after binding of the prion protein to laminin gamma1 chain. *Faseb J* **25**, 265-279
37. Benarroch, E. E. (2008) Metabotropic glutamate receptors: synaptic modulators and therapeutic targets for neurologic disease. *Neurology* **70**, 964-968
38. Rammes, G., Hasenjager, A., Sroka-Saidi, K., Deussing, J. M., and Parsons, C. G. (2011) Therapeutic significance of NR2B-containing NMDA receptors and mGluR5 metabotropic glutamate receptors in mediating the synaptotoxic effects of beta-amyloid oligomers on long-term potentiation (LTP) in murine hippocampal slices. *Neuropharmacology* **60**, 982-990
39. Wang, Q., Walsh, D. M., Rowan, M. J., Selkoe, D. J., and Anwyl, R. (2004) Block of long-term potentiation by naturally secreted and synthetic amyloid beta-peptide in hippocampal slices is mediated via activation of the kinases c-Jun N-terminal kinase, cyclin-dependent kinase 5, and p38 mitogen-activated protein kinase as well as metabotropic glutamate receptor type 5. *J Neurosci* **24**, 3370-3378
40. Bruno, V., Ksiazek, I., Battaglia, G., Lukic, S., Leonhardt, T., Sauer, D., Gasparini, F., Kuhn, R., Nicoletti, F., and Flor, P. J. (2000) Selective blockade of metabotropic glutamate receptor subtype 5 is neuroprotective. *Neuropharmacology* **39**, 2223-2230
41. Hu, N. W., Nicoll, A. J., Zhang, D., Mably, A. J., O'Malley, T., Purro, S. A., Terry, C., Collinge, J., Walsh, D. M., and Rowan, M. J. (2014) mGlu5 receptors and cellular prion protein mediate amyloid-beta-facilitated synaptic long-term depression in vivo. *Nat Commun* **5**, 3374
42. Larson, M., Sherman, M. A., Amar, F., Nuvolone, M., Schneider, J. A., Bennett, D. A., Aguzzi, A., and Lesne, S. E. (2012) The complex PrP(c)-Fyn couples human oligomeric Aβeta with pathological tau changes in Alzheimer's disease. *The Journal of neuroscience : the official journal of the Society for Neuroscience* **32**, 16857-16871a
43. Antonyuk, S. V., Trevitt, C. R., Strange, R. W., Jackson, G. S., Sangar, D., Batchelor, M., Cooper, S., Fraser, C., Jones, S., Georgiou, T., Khalili-Shirazi, A., Clarke, A. R., Hasnain, S. S., and Collinge, J. (2009) Crystal structure of human prion protein bound to a therapeutic antibody. *Proc Natl Acad Sci U S A* **106**, 2554-2558
44. Wu, H., Wang, C., Gregory, K. J., Han, G. W., Cho, H. P., Xia, Y., Niswender, C. M., Katritch, V., Meiler, J., Cherezov, V., Conn, P. J., and Stevens, R. C. (2014) Structure of a class C GPCR metabotropic glutamate receptor 1 bound to an allosteric modulator. *Science* **344**, 58-64
45. Muto, T., Tsuchiya, D., Morikawa, K., and Jingami, H. (2007) Structures of the extracellular regions of the group II/III metabotropic glutamate receptors. *Proc Natl Acad Sci U S A* **104**, 3759-3764
46. Jankowsky, J. L., Xu, G., Fromholt, D., Gonzales, V., and Borchelt, D. R. (2003) Environmental enrichment exacerbates amyloid plaque formation in a transgenic mouse model of Alzheimer disease. *J Neuropathol Exp Neurol* **62**, 1220-1227
47. Lu, Y. M., Jia, Z., Janus, C., Henderson, J. T., Gerlai, R., Wojtowicz, J. M., and Roder, J. C. (1997) Mice lacking metabotropic glutamate receptor 5 show impaired learning and reduced CA1 long-term potentiation (LTP) but normal CA3 LTP. *J Neurosci* **17**, 5196-5205
48. O'Brien, J. A., Lemaire, W., Chen, T. B., Chang, R. S., Jacobson, M. A., Ha, S. N., Lindsley, C. W., Schaffhauser, H. J., Sur, C., Pettibone, D. J., Conn, P. J., and Williams, D. L., Jr. (2003) A family of highly selective allosteric modulators of the metabotropic glutamate receptor subtype 5. *Mol Pharmacol* **64**, 731-740

49. Rondard, P., Goudet, C., Kniazeff, J., Pin, J. P., and Prezeau, L. (2011) The complexity of their activation mechanism opens new possibilities for the modulation of mGlu and GABAB class C G protein-coupled receptors. *Neuropharmacology* **60**, 82-92
50. Schwartz, T. W., Frimurer, T. M., Holst, B., Rosenkilde, M. M., and Elling, C. E. (2006) Molecular mechanism of 7TM receptor activation--a global toggle switch model. *Annu Rev Pharmacol Toxicol* **46**, 481-519
51. Ribeiro, F. M., Paquet, M., Cregan, S. P., and Ferguson, S. S. (2010) Group I metabotropic glutamate receptor signalling and its implication in neurological disease. *CNS Neurol Disord Drug Targets* **9**, 574-595
52. Pin, J. P., and Duvoisin, R. (1995) The metabotropic glutamate receptors: structure and functions. *Neuropharmacology* **34**, 1-26
53. Luscher, C., and Huber, K. M. (2010) Group 1 mGluR-dependent synaptic long-term depression: mechanisms and implications for circuitry and disease. *Neuron* **65**, 445-459
54. Um, J. W., and Strittmatter, S. M. (2013) Amyloid-beta induced signaling by cellular prion protein and Fyn kinase in Alzheimer disease. *Prion* **7**, 37-41
55. Yusa, S., Oliveira-Martins, J. B., Sugita-Konishi, Y., and Kikuchi, Y. (2012) Cellular prion protein: from physiology to pathology. *Viruses* **4**, 3109-3131
56. Pin, J. P., Galvez, T., and Prezeau, L. (2003) Evolution, structure, and activation mechanism of family 3/C G-protein-coupled receptors. *Pharmacol Ther* **98**, 325-354
57. Gregory, K. J., Dong, E. N., Meiler, J., and Conn, P. J. (2011) Allosteric modulation of metabotropic glutamate receptors: structural insights and therapeutic potential. *Neuropharmacology* **60**, 66-81
58. Sheffler, D. J., Gregory, K. J., Rook, J. M., and Conn, P. J. (2011) Allosteric modulation of metabotropic glutamate receptors. *Advances in pharmacology* **62**, 37-77
59. Gasparini, F., and Spooren, W. (2007) Allosteric modulators for mGlu receptors. *Current neuropharmacology* **5**, 187-194
60. Gregory, K. J., Noetzel, M. J., Rook, J. M., Vinson, P. N., Stauffer, S. R., Rodriguez, A. L., Emmitte, K. A., Zhou, Y., Chun, A. C., Felts, A. S., Chauder, B. A., Lindsley, C. W., Niswender, C. M., and Conn, P. J. (2012) Investigating metabotropic glutamate receptor 5 allosteric modulator cooperativity, affinity, and agonism: enriching structure-function studies and structure-activity relationships. *Mol Pharmacol* **82**, 860-875
61. Molck, C., Harpsoe, K., Gloriam, D. E., Mathiesen, J. M., Nielsen, S. M., and Brauner-Osborne, H. (2014) mGluR5: Exploration of Orthosteric and Allosteric Ligand Binding Pockets and Their Applications to Drug Discovery. *Neurochem Res*
62. Bruno, V., Battaglia, G., Copani, A., D'Onofrio, M., Di Iorio, P., De Blasi, A., Melchiorri, D., Flor, P. J., and Nicoletti, F. (2001) Metabotropic glutamate receptor subtypes as targets for neuroprotective drugs. *J Cereb Blood Flow Metab* **21**, 1013-1033
63. Trevitt, C. R., and Collinge, J. (2006) A systematic review of prion therapeutics in experimental models. *Brain* **129**, 2241-2265
64. Xu, J., Zhu, Y., Contractor, A., and Heinemann, S. F. (2009) mGluR5 has a critical role in inhibitory learning. *J Neurosci* **29**, 3676-3684
65. Wisniewski, K., and Car, H. (2002) (S)-3,5-DHPG: a review. *CNS Drug Rev* **8**, 101-116
66. Reisberg, B., Doody, R., Stoffler, A., Schmitt, F., Ferris, S., Mobius, H. J., and Memantine Study, G. (2003) Memantine in moderate-to-severe Alzheimer's disease. *N Engl J Med* **348**, 1333-1341
67. Lipton, S. A. (2005) The molecular basis of memantine action in Alzheimer's disease and other neurologic disorders: low-affinity, uncompetitive antagonism. *Current Alzheimer research* **2**, 155-165
68. Serge, A., Fourgeaud, L., Hemar, A., and Choquet, D. (2002) Receptor activation and homer differentially control the lateral mobility of metabotropic glutamate receptor 5 in the neuronal membrane. *J Neurosci* **22**, 3910-3920
69. Rosenmund, C., Feltz, A., and Westbrook, G. L. (1995) Calcium-dependent inactivation of synaptic NMDA receptors in hippocampal neurons. *J Neurophysiol* **73**, 427-430
70. Mao, L., Yang, L., Tang, Q., Samdani, S., Zhang, G., and Wang, J. Q. (2005) The scaffold protein Homer1b/c links metabotropic glutamate receptor 5 to extracellular signal-regulated protein kinase cascades in neurons. *J Neurosci* **25**, 2741-2752

71. Hou, L., and Klann, E. (2004) Activation of the phosphoinositide 3-kinase-Akt-mammalian target of rapamycin signaling pathway is required for metabotropic glutamate receptor-dependent long-term depression. *J Neurosci* **24**, 6352-6361
72. Tu, J. C., Xiao, B., Naisbitt, S., Yuan, J. P., Petralia, R. S., Brakeman, P., Doan, A., Aakalu, V. K., Lanahan, A. A., Sheng, M., and Worley, P. F. (1999) Coupling of mGluR/Homer and PSD-95 complexes by the Shank family of postsynaptic density proteins. *Neuron* **23**, 583-592
73. Leclerc, E., Liemann, S., Wildegger, G., Vetter, S. W., and Nilsson, F. (2000) Selection and characterization of single chain Fv fragments against murine recombinant prion protein from a synthetic human antibody phage display library. *Human antibodies* **9**, 207-214
74. Feraudet, C., Morel, N., Simon, S., Volland, H., Frobert, Y., Creminon, C., Vilette, D., Lehmann, S., and Grassi, J. (2005) Screening of 145 anti-PrP monoclonal antibodies for their capacity to inhibit PrP^{Sc} replication in infected cells. *J Biol Chem* **280**, 11247-11258
75. Spinner, D. S., Kascsak, R. B., Lafauci, G., Meeker, H. C., Ye, X., Flory, M. J., Kim, J. I., Schuller-Levis, G. B., Levis, W. R., Wisniewski, T., Carp, R. I., and Kascsak, R. J. (2007) CpG oligodeoxynucleotide-enhanced humoral immune response and production of antibodies to prion protein PrP^{Sc} in mice immunized with 139A scrapie-associated fibrils. *J Leukoc Biol* **81**, 1374-1385

Acknowledgments. We thank Stefano Sodi for assistance with mouse husbandry.

Disclosures. S.M.S. is a cofounder of Axerion Therapeutics, seeking to develop NgR- and PrP-based therapeutics.

FOOTNOTES

*This work was supported by grants from NIH, BrightFocus Foundation, Alzheimer's Association and Falk Medical Research Trust to S.M.S.

¹ Cellular Neuroscience, Neurodegeneration and Repair Program, Department of Neurology, Yale University School of Medicine, New Haven, Connecticut, USA.

² Graduate School of Cellular and Molecular Neuroscience, University of Tuebingen, Tuebingen, Germany.

³ L.T.H. and M.A.K contributed equally to this work.

⁴ The abbreviations used are: A β , Amyloid-beta oligomers; AD, Alzheimer's disease; ADX-47273, S-(4-fluoro-phenyl)-{3-[3-(4-fluoro-phenyl)-[1,2,4]-oxadi-azol-5-yl]-piperidin-1-yl}-methanone; BS3, Bis(sulfosuccinimidyl)suberate; DCB, 3,3'-dichloro-benzaldazine; DHPG, Dihydroxyphenylglycine; EDTA, ethylenediaminetetraacetic acid; HCl, hydrogen chloride; HEK-293 cells, human embryonic kidney-293 cells; LTD, long-term depression; LTP, long-term potentiation; LY-456236, 6-Methoxy-N-(4-methoxyphenyl)-4-quinazolinamine hydrochloride; M β CD, methyl- β -cyclodextrin; mGluR, metabotropic glutamate receptor; MTEP, 3-((2-Methyl-4-thiazolyl) ethynyl)pyridine; PBS, phosphate-buffered saline; PLC β 1, phospholipase C β 1; PrP^C, cellular prion protein; RIPA buffer, radio immuno precipitation assay buffer; SDS-PAGE, sodium dodecyl sulfate polyacrylamide gel electrophoresis; SIB-1757, 6-methyl-2-(phenylazo)pyridin-3-ol; VU-0357121, 4-Butoxy-N-(2,4-difluorophenyl)benzamide; WT, wild type

FIGURE LEGENDS

FIGURE 1: Myc-mGluR5 binds to residues 91-153 of PrP^C. A: Cell surfaces of HEK-293 cells transfected with plasmids directing the expression of either PrP^C-Fl or each of the indicated PrP^C deletion mutants were biotinylated, detergent solubilized lysates (input) were immunoblotted with anti-PrP^C and anti-PrP^C immunoprecipitates were immunoblotted with Streptavidin. B: Schematic of the PrP^C structure and deletion locations. Grey: residues 23-51; green: octa-repeat (OR); blue: residues 91-111; red: beta-sheet rich region; yellow: helix 1 (H1); purple: helix 2 (H2); orange: helix 3 (H3). The A β binding sites in PrP^C are highlighted in dark blue (residues 23-27 and 95-110), the mGluR5 binding sites are highlighted in dark red (residues 91-153). C: HEK-293 cells were transfected with either empty pcDNA3 vector, vector for Myc-mGluR5 or PrP^C-Fl (full-length), or co-transfected for either Myc-mGluR5 and PrP^C-Fl or PrP^C deletion mutants, as indicated. Detergent solubilized lysates (input), anti-Myc immunoprecipitates and anti-PrP^C immunoprecipitates were immunoblotted with either anti-Myc or anti-PrP^C, as indicated. D: The quantified PrP^C deletion mutant signal in anti-Myc immunoprecipitates is normalized to the PrP^C-Fl signal in anti-Myc immunoprecipitates. Data are mean and s.e.m. from 4 experiments. Co-immunoprecipitation of Myc-mGluR5 with PrP^C-d91-111 and Myc-mGluR5 with PrP^C-dBeta is significantly reduced ($p = 0.0059$ and $p = 0.0359$ by one-sample t-test). E: The quantified Myc signal in anti-PrP^C deletion mutant immunoprecipitates is normalized to the Myc signal in anti-PrP^C-Fl immunoprecipitates. Data are mean and s.e.m. from 4 experiments. Co-immunoprecipitation of Myc-mGluR5 with PrP^C-d91-111 ($p = 0.0023$ by one-sample t-test) and co-immunoprecipitation of Myc-mGluR5 with PrP^C-dHelix 1 is significantly reduced ($p = 0.0081$ by one-sample t-test).

FIGURE 2: Antibodies directed against region 91-153 of PrP^C block the Myc-mGluR5 binding to immobilized PrP^C. A, D-F: Relative binding of detergent solubilized Myc-mGluR to immobilized recombinant PrP^C. A: Immobilized PrP^C strongly interacts with Myc-mGluR5 lysates but not with Myc-mGluR8 lysates or control lysates. B: Myc-mGluR lysates used in A were immunoblotted with anti-Myc. C: Schematic of the PrP^C structure and antibody epitopes. Antibodies used in mapping experiments are 6D11 (epitope: 97-100), 3F4 (epitope: 108-111), Pri308 (epitope: 106-126), 6G3 (epitope: 130-150), Bar221 and Bar 233 (Bar221/3; epitope: 141-151), Saf70 (epitope 156-162), 11C6 (epitope: 142-160), M20 (epitope: C-terminal residues) (73-75). D: Antibodies recognizing region 91-

111 of PrP^C (6D11, 3F4, Pri308) disrupt the interaction between Myc-mGluR5 and immobilized PrP^C dose-dependently. E: Antibodies directed against the beta-sheet rich region and helix 1 of PrP^C (BAR233, 6G3, BAR221) blocked the Myc-mGluR5 binding to PrP^C dose-dependently. F: No disruption of the Myc-mGluR5 binding to immobilized PrP^C was initiated by control antibodies not recognizing PrP^C (GAPDH) or antibodies recognizing exclusively domains other than region 91-153 of PrP^C (SAF61, M20, 11C6).

FIGURE 3: Agonist/antagonist driven conformational states of mGluR5 regulate the interaction of HEK-293 cell expressed PrP^C and Myc-mGluR5. A: HEK-293 cells were transfected with either empty pcDNA3 vector, vector for PrP^C or Myc-mGluR5, or co-transfected for PrP^C and Myc-mGluR5. Cells were incubated for 10 min at 37°C with 2.5 μM indicated drug. Detergent solubilized lysates (input) were immunoblotted with either anti-Myc or anti-PrP^C, as indicated. Anti-Myc immunoprecipitates and anti-PrP^C immunoprecipitates were supplied with 2.5 μM indicated drug and immunoblotted with either anti-Myc or anti-PrP^C. B: Cells were incubated for 10 min at 37°C with indicated drug concentrations. One culture was pre-incubated for 10 min with 25 μM DCB prior to incubation for 10 min at 37°C with 2.5 μM MTEP. Detergent solubilized lysates (input) were immunoblotted with either anti-Myc or anti-PrP^C, as indicated. Anti-Myc immunoprecipitates and anti-PrP^C immunoprecipitates were supplied with indicated drug concentrations and immunoblotted with either anti-Myc or anti-PrP^C, as indicated. C,D: Positive allosteric modulators and agonists are shown in green, silent allosteric modulators are shown in yellow and negative allosteric modulators are shown in red. C: Quantification of the PrP^C signal in anti-Myc immunoprecipitates is normalized to the signal of untreated samples. Data are mean and s.e.m. from 4 experiments, apart from DHPG, DCB and MTEP application from 11, 6 and 12 independent experiments, respectively. Co-immunoprecipitation of PrP^C with Myc-mGluR5 is significantly enhanced by DHPG ($p = 0.00049$ by Wilcoxon Signed Rank Test), and significantly reduced by MTEP ($p = 0.00024$ by Wilcoxon Signed Rank Test). On the contrary, LY-456236 hydrochloride, a selective mGluR1 receptor antagonist, did not significantly alter the PrP^C signal in anti-Myc immunoprecipitates. D: Quantification of the Myc signal in anti-PrP^C immunoprecipitates after treatment is normalized to the signal of untreated samples. Data are mean and s.e.m. from 4 experiments, apart from DHPG and MTEP application from 11 independent experiments. Co-immunoprecipitation of Myc-mGluR5 with PrP^C is significantly enhanced by DHPG ($p = 0.00098$ by Wilcoxon Signed Rank Test), and significantly reduced by MTEP ($p = 0.00049$ by Wilcoxon Signed Rank Test). In contrast, LY-456236 hydrochloride did not significantly change the Myc signal in anti-PrP^C immunoprecipitates.

FIGURE 4: Antagonist driven conformational states of mGluR5 regulate the interaction of HEK-293 cell expressed PrP^C and Myc-mGluR5 in a dose-dependent manner. A: HEK-293 cells were co-transfected for PrP^C and Myc-mGluR5. Cells were incubated for 10 min at 37°C with indicated MTEP concentration and detergent solubilized lysates (input) were immunoblotted with either anti-Myc or anti-PrP^C, as indicated. Anti-Myc immunoprecipitates and anti-PrP^C immunoprecipitates were supplied with indicated MTEP concentration and immunoblotted with either anti-Myc or anti-PrP^C, as indicated. B: Quantification of the PrP^C signal in anti-Myc immunoprecipitates after treatment is normalized to the signal of untreated samples. Data are mean and s.e.m. from 4 experiments, apart from 2.5 μM MTEP application from 11 independent experiments. Co-immunoprecipitation of PrP^C with Myc-mGluR5 is significantly reduced by MTEP (****: $P < 0.0001$; ***: $P < 0.001$; **: $P < 0.01$; *: $P < 0.05$; one-sample t-test). C: Quantification of the Myc signal in anti-PrP^C immunoprecipitates after treatment is normalized to the signal of untreated samples. Data are mean and s.e.m. from 4 experiments, apart from 2.5 μM MTEP application from 10 experiments. Co-immunoprecipitation of Myc-mGluR5 with PrP^C is significantly reduced by MTEP (****: $P < 0.0001$; ***: $P < 0.001$; **: $P < 0.01$; *: $P < 0.05$; one-sample t-test).

FIGURE 5: Agonist/antagonist driven conformational states of mGluR5 regulate the interaction of PrP^C with Myc-mGluR5 but not PrP^C with Myc-mGluR8 and only partially of PrP^C with chimeric Myc-mGluR proteins. A: Schematics showing the design of Myc-tagged mGluR mutants and location of ligand binding. B: HEK-293 cells were co-transfected with vectors for PrP^C and different Myc-tagged mGluRs, as indicated. Cells were incubated for 10 min at 37°C with 100 μM glutamate or 2.5 μM indicated drug and detergent solubilized lysates (input) were immunoblotted with either anti-Myc

or anti-PrP^C, as indicated. Anti-Myc immunoprecipitates and anti-PrP^C immunoprecipitates were incubated with 100 μ M glutamate or 2.5 μ M indicated drug and immunoblotted with either anti-Myc or anti-PrP^C, as indicated. C: Quantification of the PrP^C signal in anti-Myc immunoprecipitates is normalized to the PrP^C signal in anti-Myc-mGluR5 immunoprecipitates. Data are mean and s.e.m. from 4 experiments. The PrP^C signal in anti-Myc-mGluR8 immunoprecipitates ($p = 0.0006$ by one-sample t-test) and in Myc-mGluR-N5/C8 immunoprecipitates ($p = 0.0329$ by one-sample t-test) is significantly reduced. D: Quantification of the Myc signal in anti-PrP^C immunoprecipitates is normalized to the Myc-mGluR5 signal in anti-PrP^C immunoprecipitates. Data are mean and s.e.m. from 4 experiments. Interaction of Myc-mGluR8 and PrP^C is significantly reduced ($p = 0.0005$ by one-sample t-test). E, G, I: Quantification of the PrP^C signal in anti-Myc immunoprecipitates is normalized to the signal of untreated samples. Data are mean and s.e.m. from 2-10 experiments. F, H, J: Quantification of the Myc signal in anti-PrP^C immunoprecipitates is normalized to the signal of untreated samples. E: Co-immunoprecipitation of PrP^C with Myc-mGluR5 is significantly enhanced by glutamate ($p = 0.0313$ by Wilcoxon Signed Rank Test) and DHPG ($p = 0.0020$ by Wilcoxon Signed Rank Test), and significantly reduced by MTEP ($p = 0.0020$ by Wilcoxon Signed Rank Test). F: Co-immunoprecipitation of Myc-mGluR5 with PrP^C is significantly enhanced by glutamate ($p = 0.0313$ by Wilcoxon Signed Rank Test) and DHPG ($p = 0.0020$ by Wilcoxon Signed Rank Test), and significantly reduced by MTEP ($p = 0.0020$ by Wilcoxon Signed Rank Test). G: Co-immunoprecipitation of PrP^C with Myc-mGluR-N5/C8 is not significantly altered by conformational mGluR changes due to low sample size ($n = 2$). However, a trend is clearly observable. H: Co-immunoprecipitation of Myc-mGluR-N5/C8 with PrP^C is significantly enhanced by glutamate ($p = 0.0332$ by one-sample t-test) and DHPG ($p = 0.0492$ by one-sample t-test), but not altered by MTEP. I: Co-immunoprecipitation of PrP^C with Myc-mGluR-N8/C5 is significantly reduced by MTEP ($p = 0.05$ by one-sample t-test). J: Co-immunoprecipitation of Myc-mGluR-N8/C5 with PrP^C is significantly enhanced by glutamate ($p = 0.0421$ by one-sample t-test).

FIGURE 6: The modulatory effect of agonist/antagonist driven changes on the interaction of PrP^C with Myc-mGluR5 is strongest after treatment of HEK-293 cell membrane preparations. HEK-293 cells were co-transfected with vectors for PrP^C and Myc-mGluR5. A: Cells were incubated for 10 min at 37°C with 2.5 μ M indicated drug and detergent solubilized lysates (input) were immunoblotted with either anti-Myc or anti-PrP^C, as indicated. Anti-Myc immunoprecipitates and anti-PrP^C immunoprecipitates were supplied with 2.5 μ M indicated drug and immunoblotted with either anti-Myc or anti-PrP^C, as indicated. B: Membrane fractions were prepared in absence of SDS and incubated for 3 hours at 4°C with 2.5 μ M indicated drug and membrane proteins extracted by NP-40 and membrane extractions (input). Anti-Myc immunoprecipitates and anti-PrP^C immunoprecipitates of membrane extractions were immunoblotted with either anti-Myc or anti-PrP^C, as indicated. C: Cells were incubated for 10 min at 37°C with 2.5 μ M indicated drug and detergent solubilized lysates (input), anti-Myc immunoprecipitates and anti-PrP^C immunoprecipitates were immunoblotted with either anti-Myc or anti-PrP^C, as indicated. D: Detergent solubilized cell lysates were supplied with 2.5 μ M indicated compound and detergent solubilized lysates (input), anti-Myc immunoprecipitates and anti-PrP^C immunoprecipitates were immunoblotted with either anti-mGluR5 or anti-PrP^C, as indicated.

FIGURE 7: Agonist/antagonist driven conformational states of mGluR5 regulate the interaction of PrP^C with mGluR5 in brain-derived membrane fractions. Each immunoprecipitation was performed from one Grm5^{-/-}, Prnp^{-/-} or WT mouse brain hemisphere. For each experiment, 1.5 WT brain hemispheres were combined and 3 membrane pellets prepared to ensure an equal amount of protein in each membrane aliquot. Membrane fractions were prepared in absence of SDS and incubated over night at 4°C with 2.5 μ M indicated drug. Membrane proteins were extracted by NP-40 and membrane extractions (input) and anti-PrP^C immunoprecipitates of membrane extractions were immunoblotted with either anti-mGluR5 or anti-PrP^C, as indicated. A: Membrane extractions cleared by high-speed ultracentrifugation spin did not show an agonist/antagonist dependent regulation of the mGluR5 signal in anti-PrP^C immunoprecipitates. B: Membrane extractions cleared by low-speed microcentrifugation spin showed an agonist/antagonist dependent regulation of the mGluR5 signal in anti-PrP^C immunoprecipitates. C: The quantified mGluR5 dimer and monomer signal in anti-PrP^C immunoprecipitates from membrane extractions cleared by low-speed microcentrifugation spin was

combined, since the ratio between dimer and monomer was not changed by treatment. The signal in anti-PrP^C immunoprecipitates after treatment is normalized to the signal of untreated samples. Data are mean and s.e.m. from 4 individual experiments, i.e. from 6 WT brains total, with one immunoprecipitation being performed from one hemisphere each. Co-immunoprecipitation of mGluR5 with PrP^C is significantly reduced by MTEP ($p = 0.0104$ by one-sample t-test), and significantly enhanced by DHPG ($p = 0.0116$ by one-sample t-test).

FIGURE 8: The endogenous ligands glutamate and A β enhance the interaction of PrP^C with Myc-mGluR5 in a similar manner as agonist DHPG. A: HEK-293 cells were co-transfected for PrP^C and Myc-mGluR5 and incubated for 10 min at 37°C with 100 μ M glutamate, 1 μ M A β or 2.5 μ M drug, as indicated. Some cultures were pre-incubated for 10 min with 2.5 μ M of indicated drug prior to incubation for 10 min at 37°C with 1 μ M A β or 100 μ M glutamate. Detergent solubilized lysates (input) were immunoblotted with either anti-Myc or anti-PrP^C, as indicated. Anti-Myc immunoprecipitates and anti-PrP^C immunoprecipitates were treated with 100 μ M glutamate, 1 μ M A β , 2.5 μ M drug, or a combination of ligand and drug, as indicated, and immunoblotted with either anti-Myc or anti-PrP^C, as indicated. B. Quantification of the PrP^C signal in anti-Myc immunoprecipitates after treatment is normalized to the signal of untreated samples. Data are mean and s.e.m. from 4-12 experiments. Co-immunoprecipitation of PrP^C with Myc-mGluR5 is significantly enhanced by glutamate ($p = 0.0156$ by Wilcoxon Signed Rank Test), A β ($p = 0.0119$ by Wilcoxon Signed Rank Test) and DHPG ($p = 0.00049$ by Wilcoxon Signed Rank Test), and significantly reduced by MTEP ($p = 0.00024$ by Wilcoxon Signed Rank Test). Co-immunoprecipitation of PrP^C with Myc-mGluR5 in cells pre-incubated with MTEP prior to A β is not significantly different to the co-immunoprecipitation of PrP^C with Myc-mGluR5 in untreated cells. C: Quantification of the Myc signal in anti-PrP^C immunoprecipitates after treatment is normalized to the signal of untreated samples. Data are mean and s.e.m. from 4-11 experiments. Co-immunoprecipitation of Myc-mGluR5 with PrP^C is significantly enhanced by glutamate ($p = 0.0156$ by Wilcoxon Signed Rank Test), A β ($p = 0.0312$ by Wilcoxon Signed Rank Test) and DHPG ($p = 0.00098$ by Wilcoxon Signed Rank Test), and significantly reduced by MTEP ($p = 0.00049$ by Wilcoxon Signed Rank Test). Co-immunoprecipitation of Myc-mGluR5 with PrP^C in cells pre-incubated with MTEP prior to A β is not significantly different to the co-immunoprecipitation of these proteins in untreated cells.

FIGURE 9: A β -induced enhancement of the co-immunoprecipitation of PrP^C with mGluR5 requires intact lipid rafts. A. HEK-293 cells were co-transfected for PrP^C and Myc-mGluR5 and incubated for 1 hour at 37°C with 5 mg ml⁻¹ M β CD prior to 1 μ M A β exposure for 10 min at 37°C. Detergent solubilized lysates (input) were immunoblotted with either anti-Myc or anti-PrP^C, as indicated. Anti-Myc immunoprecipitates and anti-PrP^C immunoprecipitates were treated with 1 μ M A β and immunoblotted with either anti-Myc or anti-PrP^C, as indicated. B. Quantification of the PrP^C signal in anti-Myc immunoprecipitates after A β exposure is normalized to the signal of vehicle treated samples. Data are mean and s.e.m. from 3 experiments. Co-immunoprecipitation of PrP^C with Myc-mGluR5 is significantly enhanced by A β ($p = 0.0234$ by Wilcoxon Signed Rank Test). Co-immunoprecipitation of PrP^C with Myc-mGluR5 in cells pre-incubated with M β CD prior to A β is not significantly different to the co-immunoprecipitation of PrP^C with Myc-mGluR5 in vehicle treated cells. C: Quantification of the Myc signal in anti-PrP^C immunoprecipitates after treatment is normalized to the signal of vehicle treated samples. Data are mean and s.e.m. from 3 experiments. Co-immunoprecipitation of Myc-mGluR5 with PrP^C is significantly enhanced by A β ($p = 0.0313$ by Wilcoxon Signed Rank Test). Co-immunoprecipitation of Myc-mGluR5 with PrP^C in cells pre-incubated with M β CD prior to A β is not significantly different to the co-immunoprecipitation of these proteins in untreated cells.

FIGURE 10: A β -induced enhancement of the co-immunoprecipitation of PrP^C with mGluR5 in membrane fractions can be reversed by mGluR5-directed antagonists and antibodies directed against region 91-153 of PrP^C. A: HEK-293 cells were co-transfected for PrP^C and Myc-mGluR5. Membrane fractions were prepared in absence of SDS and incubated for 3 hours at 4°C with either 2.5 μ M MTEP, 25 μ M DCB, 0.1 μ M antibody, 1 μ M A β , or a combination of A β and therapeutic molecule, as indicated. Membrane proteins were extracted by NP-40 and membrane extractions (input) and anti-

Myc immunoprecipitates (using Goat Anti-Rabbit IgG Magnetic Beads) of membrane extractions were immunoblotted with either anti-Myc or anti-PrP^C. B,C: Quantification of the PrP^C signal in anti-Myc immunoprecipitates after treatment is normalized to the signal of untreated samples. B: Data are mean and s.e.m. from 5-12 experiments. Co-immunoprecipitation of PrP^C with Myc-mGluR5 is significantly reduced by MTEP ($p = 0.00098$ by Wilcoxon Signed Rank Test) and significantly enhanced by A β ($p = 0.0234$ by Wilcoxon Signed Rank Test). C: Data are mean and s.e.m. from 3-8 experiments. Co-immunoprecipitation of Myc-mGluR5 with PrP^C is significantly enhanced by A β ($p = 0.0234$ by Wilcoxon Signed Rank Test). This augmentation can be reversed by simultaneous incubation with MTEP, DCB, 6D11 and Bar 221 to a level that is not significantly different to untreated samples.

FIGURE 11: The co-immunoprecipitation of PrP^C with mGluR5 is dramatically enhanced in APP/PS1⁺ mice brain or WT brain incubated with A β , which can be reversed by mGluR5-directed antagonists and PrP^C-directed antibodies. A: Brain lysates from WT and APP/PS1⁺ mice were immunoblotted with either anti-mGluR5, anti-PrP^C, or anti-APP, as indicated. Actin is loading control. B: 2 WT brain homogenizations and 2 APP/PS1⁺ brain homogenizations were combined and 4 membrane fractions prepared in absence of SDS for each genotype to ensure an equal amount of protein in either WT or APP/PS1⁺ brain membrane aliquot. Membrane fractions were treated overnight at 4°C with either 1 μ M A β , 2.5 μ M MTEP, 25 μ M DCB, 0.1 μ M antibody, or a combination of A β and therapeutic molecule, as indicated. Membrane proteins were extracted by NP-40. Membrane extractions (input) and anti-PrP^C immunoprecipitates (using Saf32-crosslinked protein A/G coupled-beads) of membrane extractions were immunoblotted with either anti-mGluR5, anti-PrP^C, or anti-APP, as indicated. Actin is loading control. C: Quantification of the combined mGluR5 dimer and monomer signal in anti-PrP^C immunoprecipitates is normalized to actin. Data are mean and s.e.m. from 9 individual 4-13 months old animals per genotype. The mGluR5 signal in anti-PrP^C immunoprecipitates is significantly increased in APP/PS1⁺ brain ($p = 0.0005$ by Mann-Whitney test). D: The combined mGluR5 dimer and monomer signal in anti-PrP^C immunoprecipitates after treatment is normalized to the signal of untreated samples. Data are mean and s.e.m. from 3 individual experiments, one experiment performed from 2 wt and 2 APP/PS1⁺ brain each, as described above. The mGluR5 signal in anti-PrP^C immunoprecipitates of A β -treated brain-derived membrane extractions is increased in comparison to untreated membrane extractions. This enhanced mGluR5-PrP^C co-immunoprecipitation signal is significantly reduced by MTEP ($p = 0.0073$ by one-sample t-test). The mGluR5 signal in anti-PrP^C immunoprecipitates is significantly increased in APP/PS1⁺ brain-derived membrane extractions in comparison to WT brain-derived membrane extractions ($p = 0.0039$ by Wilcoxon Signed Rank Test). The mGluR5 signal in anti-PrP^C immunoprecipitates derived from MTEP treated APP/PS1⁺ membrane preparations is significantly reduced, compared to untreated APP/PS1⁺ membrane preparations ($p = 0.0024$ by one-sample t-test). The co-immunoprecipitation of mGluR5 with PrP^C is significantly reduced in 6D11 treated APP/PS1⁺ membrane preparations, in comparison to untreated APP/PS1⁺ membrane preparations ($p = 0.0053$ by one-sample t-test).

Figure 1

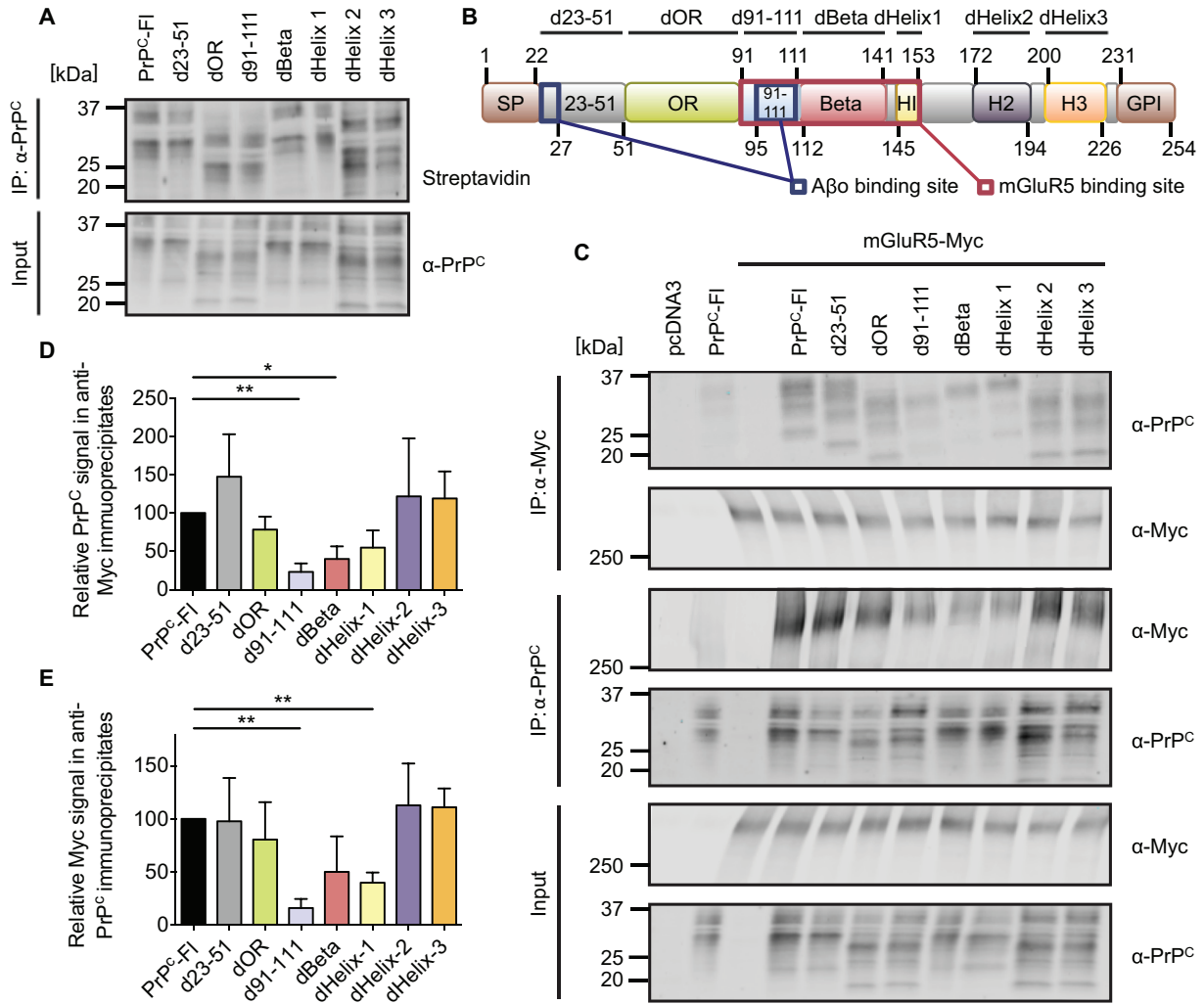


Figure 2

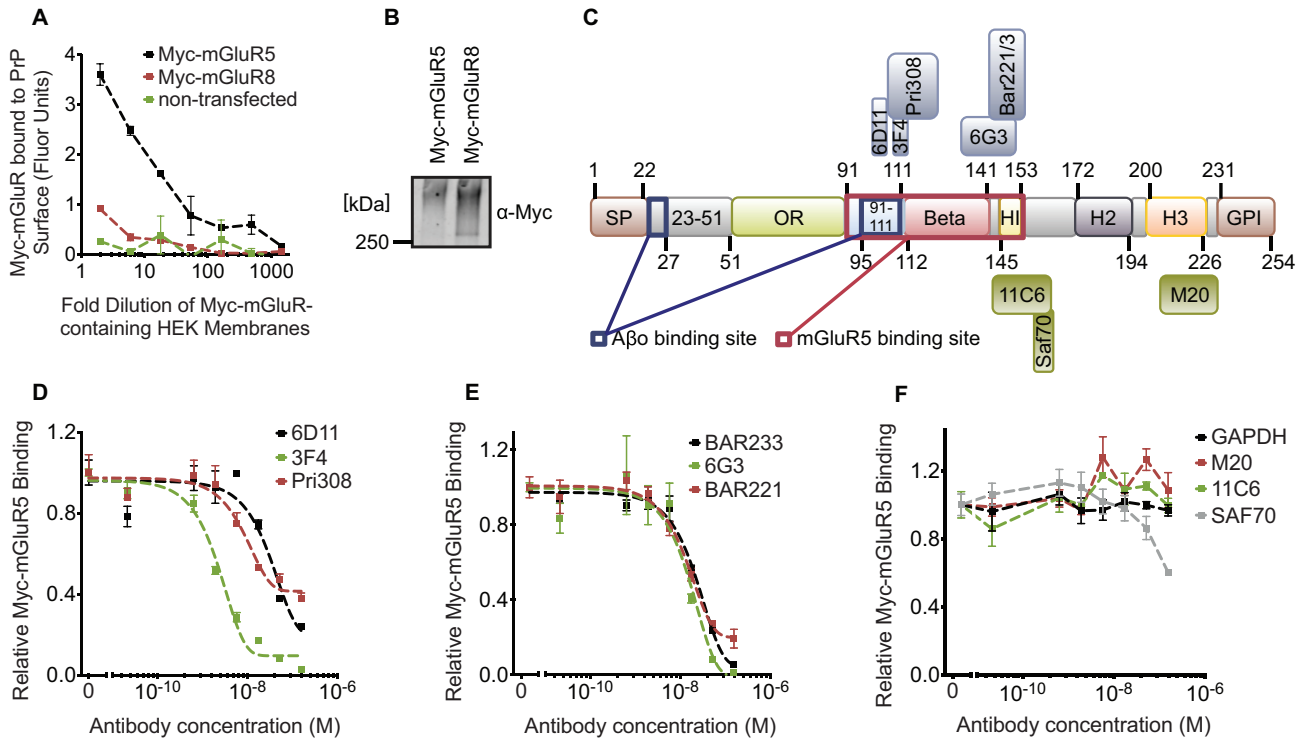


Figure 3

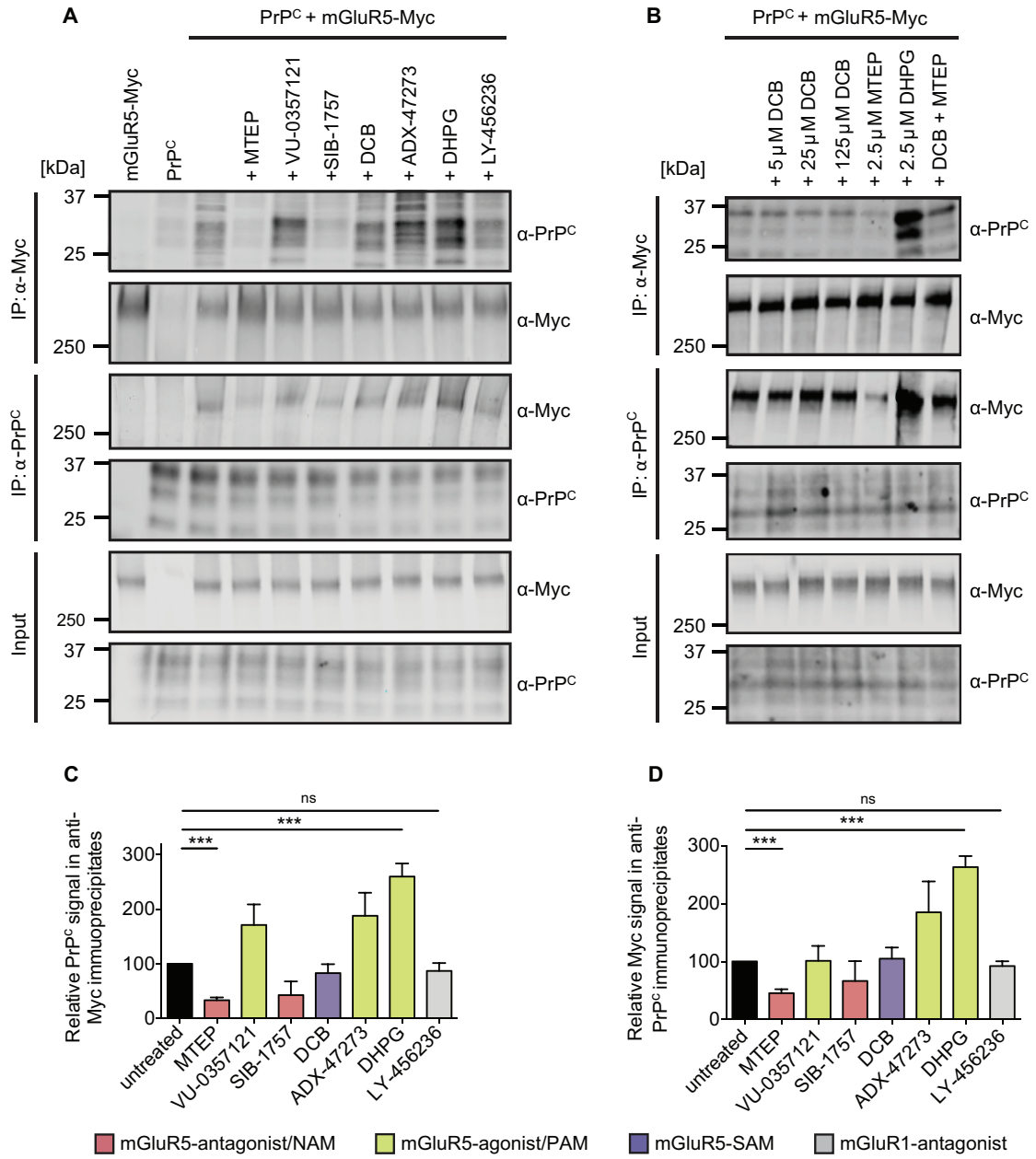


Figure 4

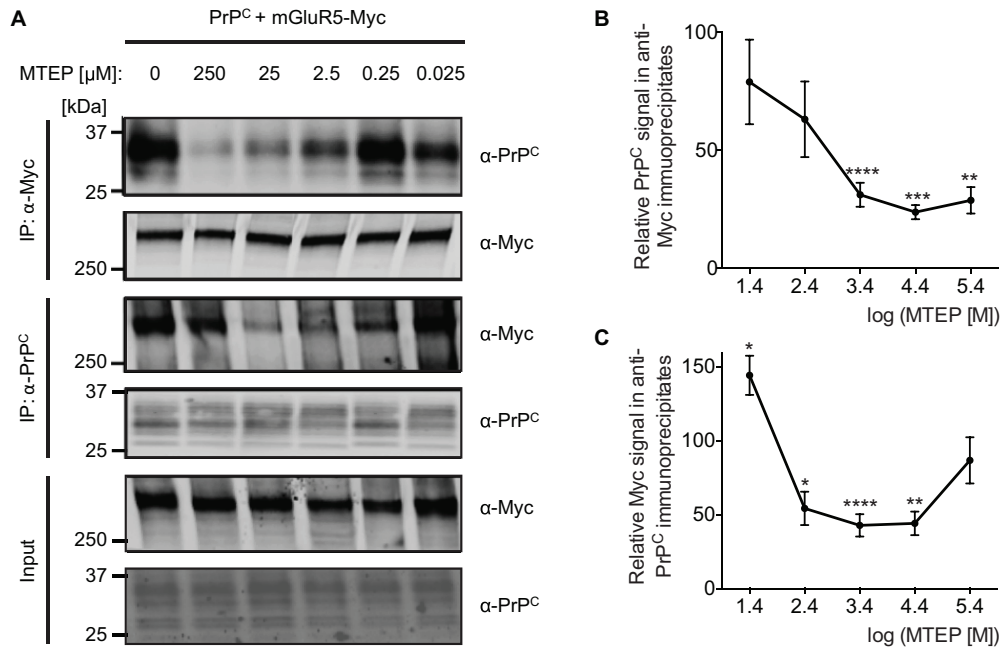


Figure 5

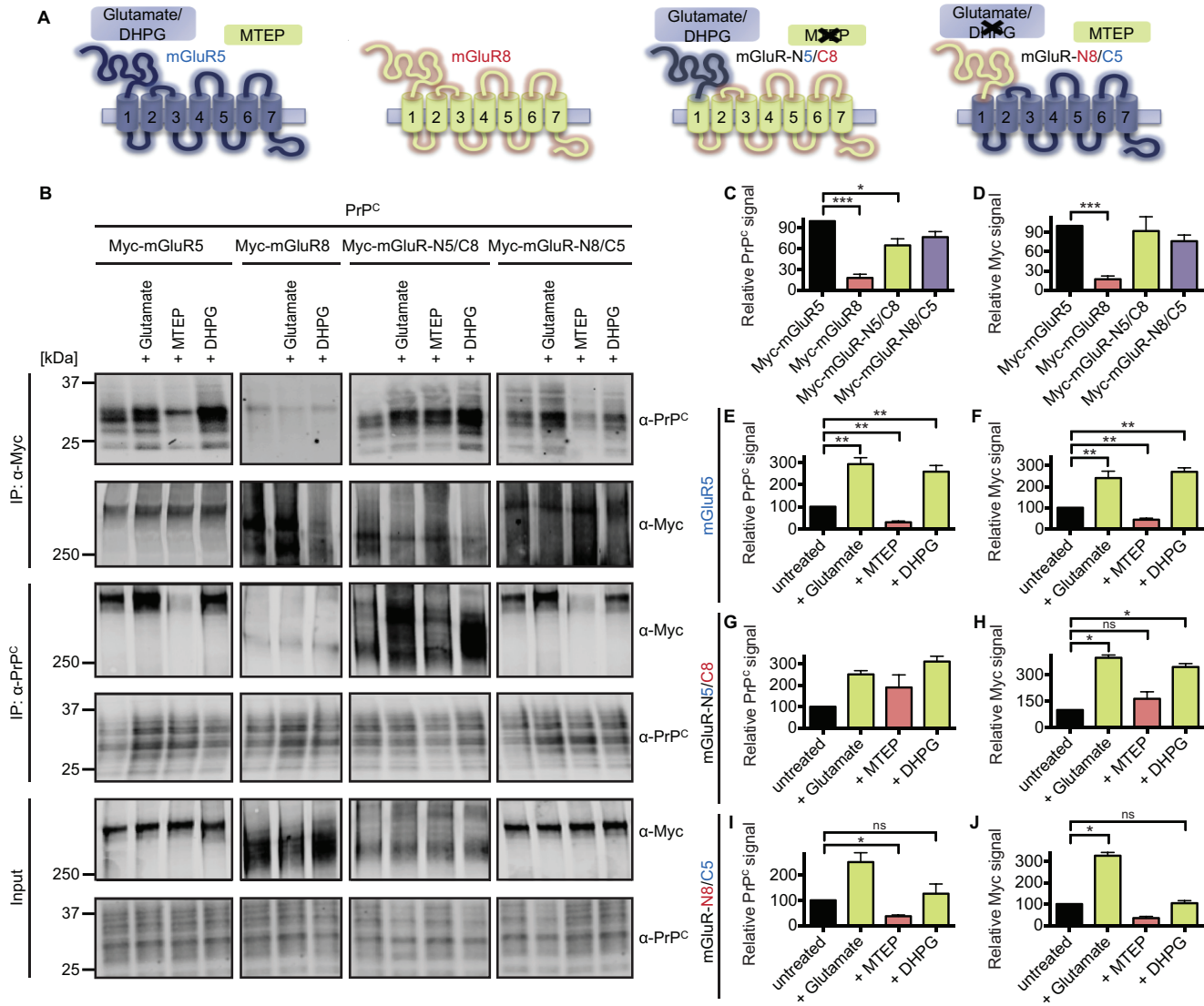


Figure 6

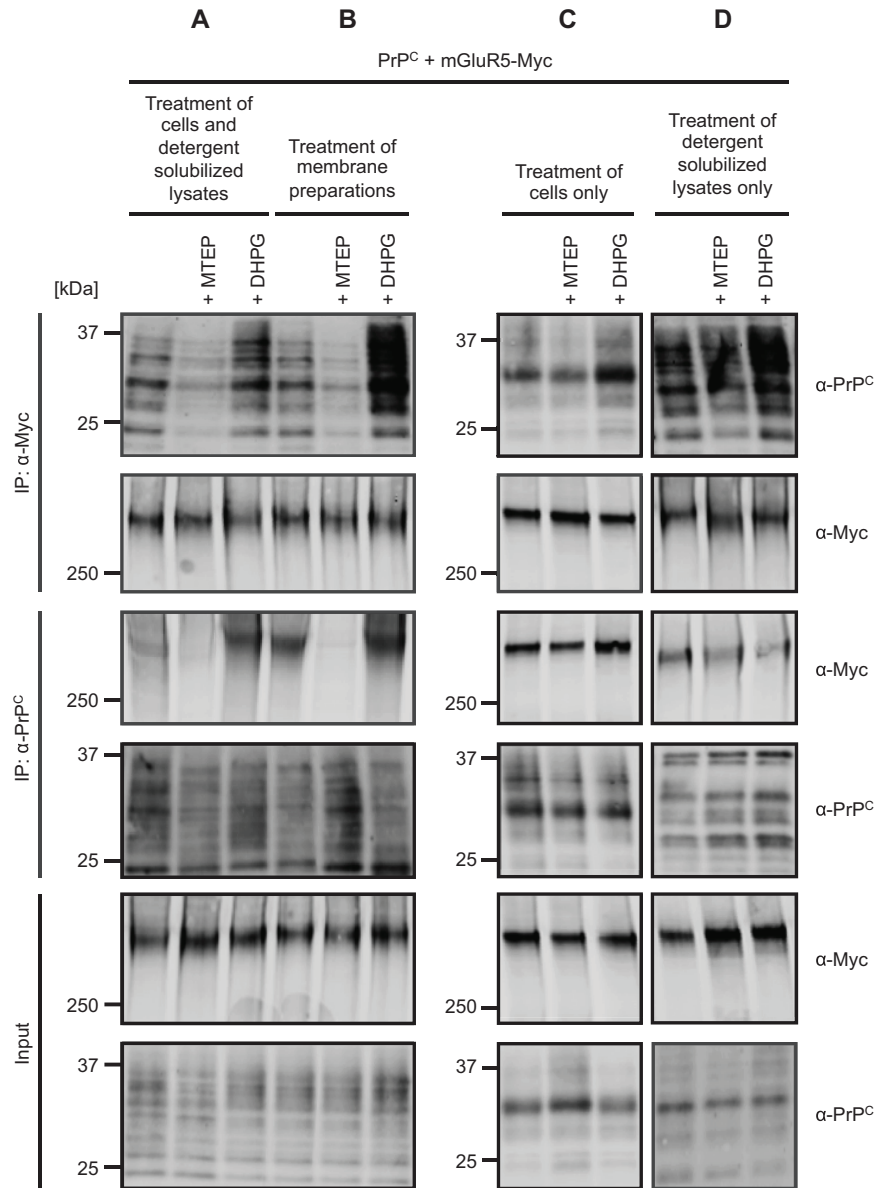


Figure 7

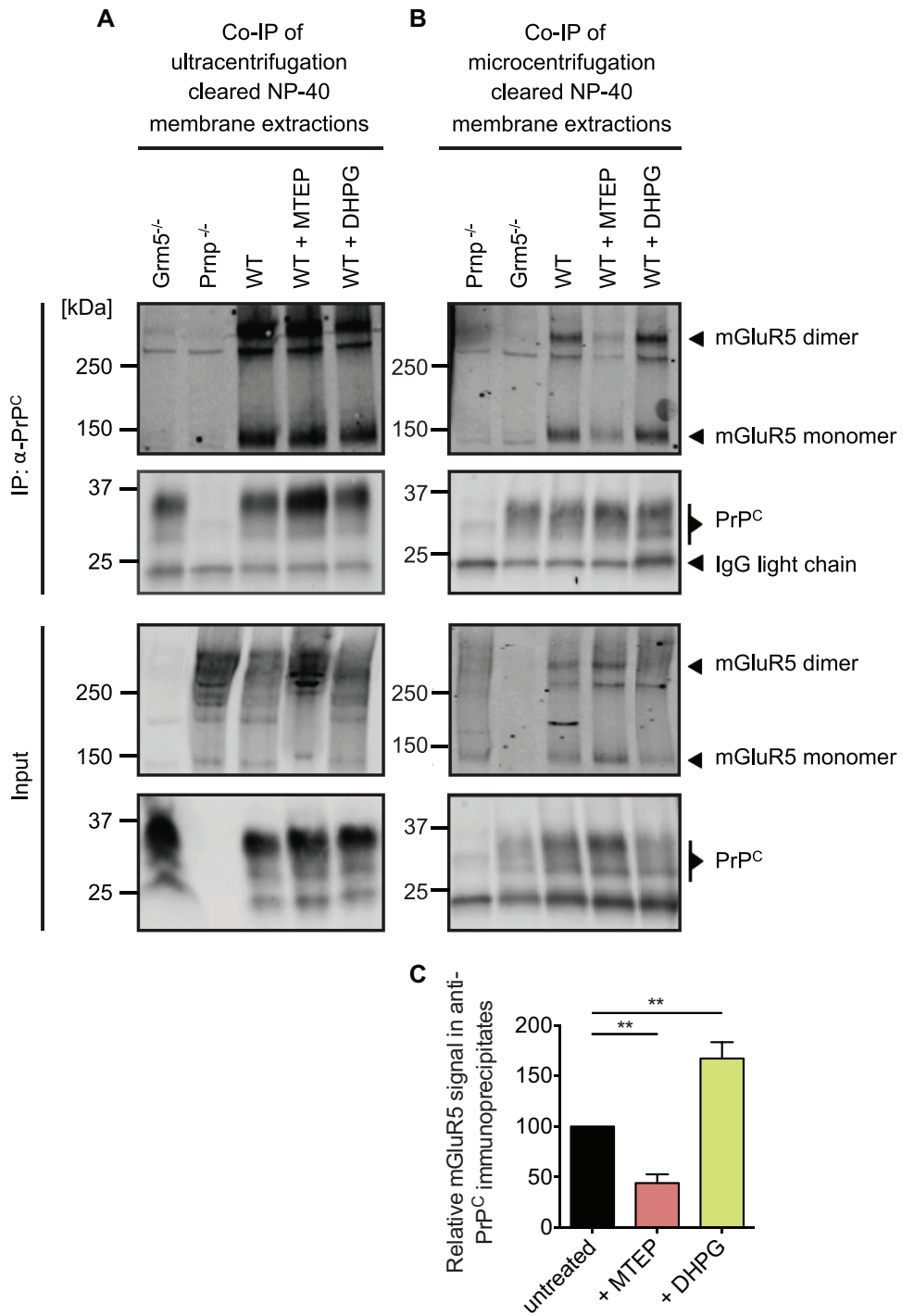


Figure 8

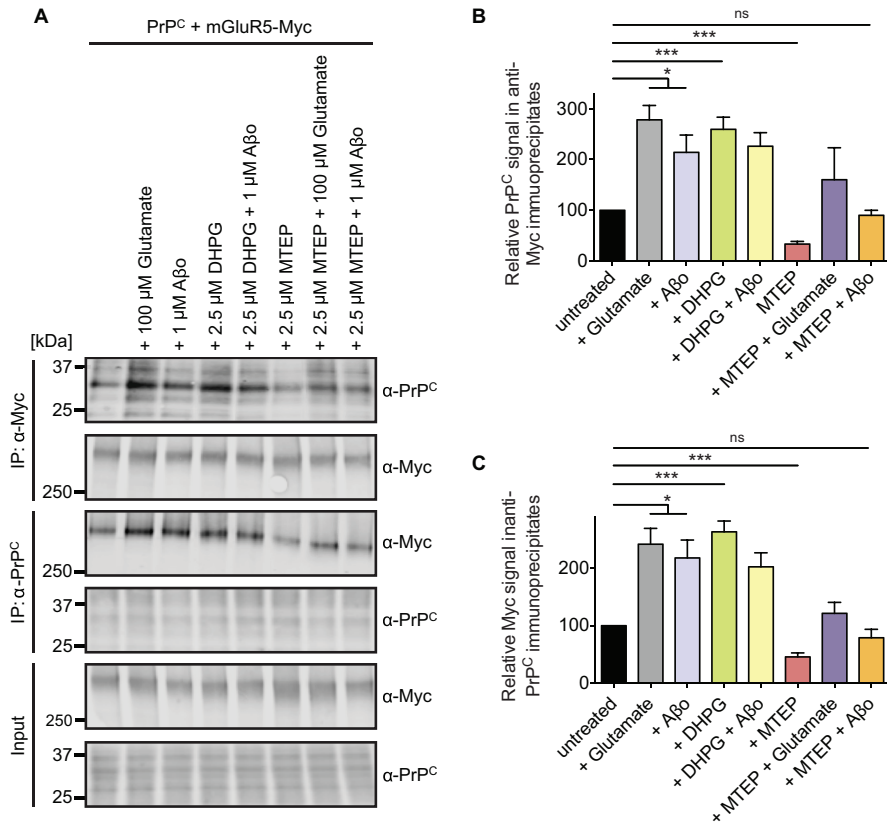


Figure 9

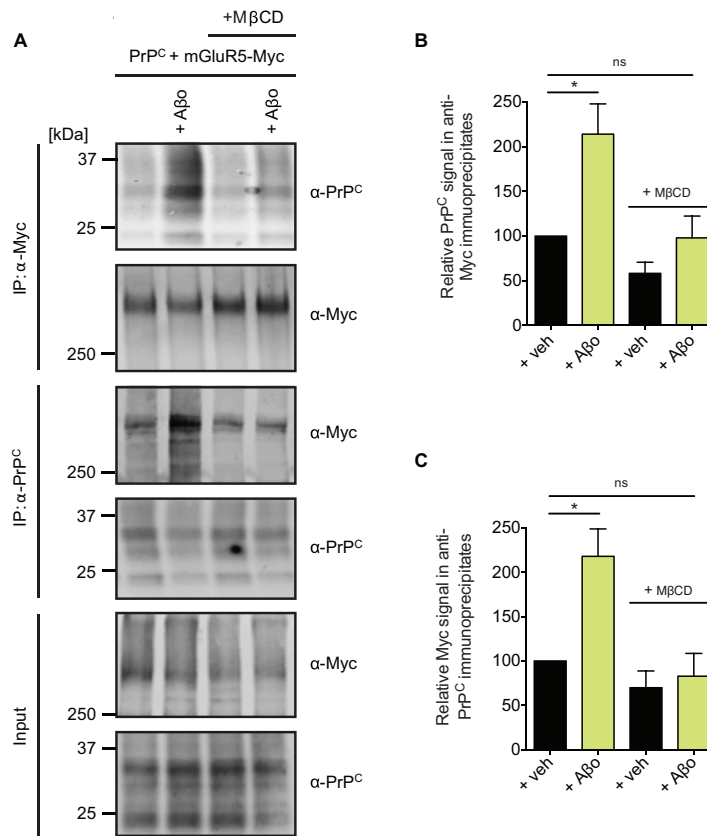


Figure 10

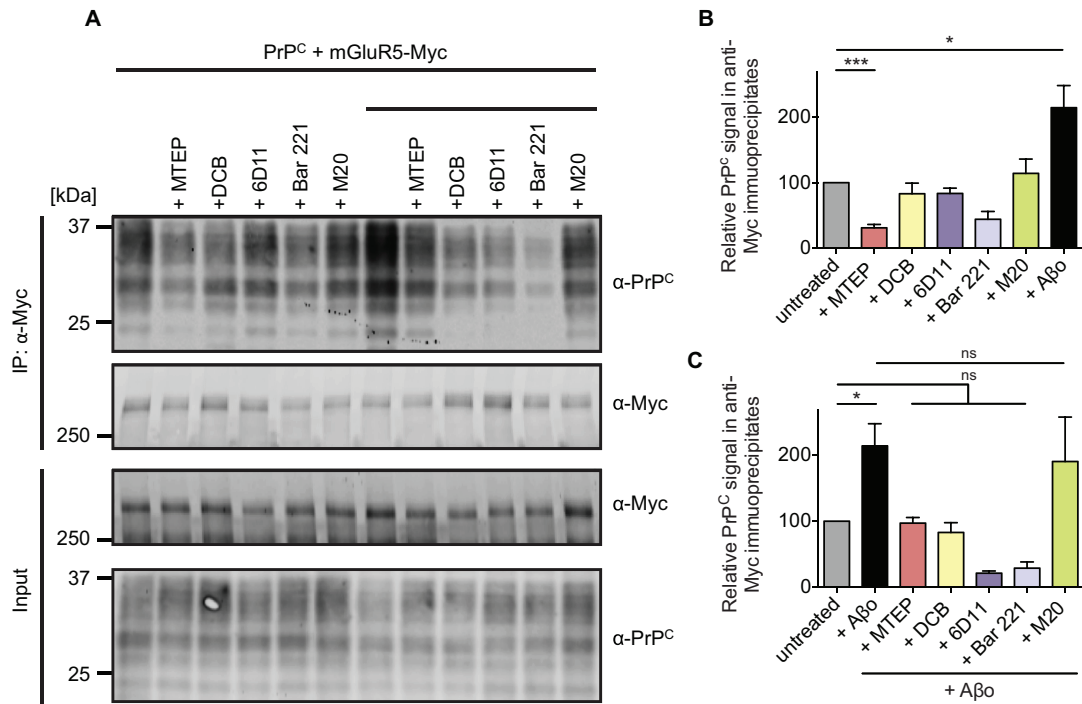


Figure 11

